NAVAL POSTGRADUATE SCHOOL

MONTEREY, CALIFORNIA

THESIS

BALLISTIC MISSILE TRAJECTORY ESTIMATION

by

Joseph Dituri

December 2006

Thesis Advisor:	Kyle T. Alfriend
Co-Advisor:	Don A. Danielson

Approved for public release; distribution is unlimited

THIS PAGE INTENTIONALLY LEFT BLANK

REPORT DOCUMENTATION PAGE		Form Approved OMB No. 0704-0188

1. AGENCY USE ONLY *(Leave blank)*	2. REPORT DATE	3. REPORT TYPE AND DATES COVERED
	December 2006	Master's Thesis

4. TITLE AND SUBTITLE	5. FUNDING NUMBERS
Ballistic Missile Trajectory Estimation	
6. AUTHOR(S) Joseph Dituri	
7. PERFORMING ORGANIZATION NAME(S) AND ADDRESS(ES) Naval Postgraduate School Monterey, CA 93943-5000	**8. PERFORMING ORGANIZATION REPORT NUMBER**
9. SPONSORING /MONITORING AGENCY NAME(S) AND ADDRESS(ES) N/A	**10. SPONSORING/MONITORING AGENCY REPORT NUMBER**

11. SUPPLEMENTARY NOTES The views expressed in this thesis are those of the author and do not reflect the official policy or position of the Department of Defense or the U.S. Government.

12a. DISTRIBUTION / AVAILABILITY STATEMENT	12b. DISTRIBUTION CODE
Approved for public release; distribution is unlimited.	A

13. ABSTRACT

Angles measurements from optical systems are the primary source of data for maintaining the orbits of high altitude satellites. Radar measurements are used primarily for low Earth orbit (LEO) satellites. Recently it has been shown that the accuracy of the orbit updates using only optical system angles-only data is just as good, if not better, than the performance from radar systems for LEO satellites. The purpose of this thesis is to investigate the use of optical angles data with and without laser ranging data in determining the trajectories of missiles. Analytical Graphics, Inc. Satellite Tool Kit is used to model the trajectory of a ballistic missile. Several scenarios are developed for determining the orbit when acquired by sensors providing various combinations of range, range rate and angles data. It is found that the combination of range, azimuth and elevation sensor data yields an orbit determination that has enough merit to be called accurate. The error of the orbit determined by the angles-only data is two orders of magnitude larger than the error of the range and angles measurement.

Additionally completed was an analysis of what would happen if the sensors could only track to the maximum altitude of the orbit. As was assumed, the known position of the object drifts ranged from minimal to significant predicated on the final known position. This is indicated by the error ellipsoid. It was again found that the combination of range, azimuth and elevation sensor data until the maximum altitude yields an orbit determination that has enough merit to be called accurate.

Also considered was the addition of a second sensor that had the capacity to always track range, azimuth and elevation to increase the time that is afforded to track the object, increasing the overall accuracy of the orbit determination. It is found that the addition of a second sensor increases the fidelity of the angles-only measurement such that the combination of azimuth and elevation sensor data yields an orbit determination that has enough merit to be called accurate.

14. SUBJECT TERMS	15. NUMBER OF PAGES
Telescope, Orbit Determination, Missile Trajectory, Highly Eccentric Orbit, Orbit determination Tool Kit, Satellite Tool Kit, MSSS, Reentry vehicle, Orbit prediction	77
	16. PRICE CODE

17. SECURITY CLASSIFICATION OF REPORT	18. SECURITY CLASSIFICATION OF THIS PAGE	19. SECURITY CLASSIFICATION OF ABSTRACT	20. LIMITATION OF ABSTRACT
Unclassified	Unclassified	Unclassified	UL

NSN 7540-01-280-5500 Standard Form 298 (Rev. 2-89)
Prescribed by ANSI Std. 239-18

THIS PAGE INTENTIONALLY LEFT BLANK

Approved for public release; distribution is unlimited

BALLISTIC MISSILE TRAJECTORY ESTIMATION

Joseph Dituri
Lieutenant Commander, United States Navy
A.S., City University of Washington, 1992
B.S., University of South Carolina, 1995

Submitted in partial fulfillment of the
requirements for the degree of

MASTER OF SCIENCE IN ASTRONAUTICAL ENGINEERING

from the

NAVAL POSTGRADUATE SCHOOL
December 2006

Author: Joseph Dituri

Approved by: Kyle T. Alfriend
Thesis Advisor

Don A. Danielson
Co-Advisor

Anthony J. Healey
Chairman, Department of Mechanical and Astronautical Engineering

THIS PAGE INTENTIONALLY LEFT BLANK

ABSTRACT

Angles measurements from optical systems are the primary source of data for maintaining the orbits of high altitude satellites. Radar measurements are used primarily for low Earth orbit (LEO) satellites. Recently it has been shown that the accuracy of the orbit updates using only optical system angles-only data is just as good, if not better, than the performance from radar systems for LEO satellites. The purpose of this thesis is to investigate the use of optical angles data with and without laser ranging data in determining the trajectories of missiles. Analytical Graphics, Inc. Satellite Tool Kit is used to model the trajectory of a ballistic missile. Several scenarios are developed for determining the orbit when acquired by sensors providing various combinations of range, range rate and angles data. It is found that the combination of range, azimuth and elevation sensor data yields an orbit determination that has enough merit to be called accurate. The error of the orbit determined by the angles-only data is two orders of magnitude larger than the error of the range and angles measurement.

Additionally completed was an analysis of what would happen if the sensors could only track to the maximum altitude of the orbit. As was assumed, the known position of the object drifts ranged from minimal to significant predicated on the final known position. This is indicated by the error ellipsoid. It was again found that the combination of range, azimuth and elevation sensor data until the maximum altitude yields an orbit determination that has enough merit to be called accurate.

Also considered was the addition of a second sensor that had the capacity to always track range, azimuth and elevation to increase the time that is afforded to track the object, increasing the overall accuracy of the orbit determination. It is found that the addition of a second sensor increases the fidelity of the angles-only measurement such that the combination of azimuth and elevation sensor data yields an orbit determination that has enough merit to be called accurate.

THIS PAGE INTENTIONALLY LEFT BLANK

TABLE OF CONTENTS

THIS PAGE INTENTIONALLY LEFT BLANK

LIST OF FIGURES

LIST OF TABLES

THIS PAGE INTENTIONALLY LEFT BLANK

LIST OF ABBREVIATIONS AND ACRONYMS

AEGIS	Mythological shield of Zeus
AEOS	Advanced Electro-Optical System
AGI	Analytical Graphics Inc
BMD	Theater Ballistic Missile Defense
EKS	Extended Kalman filter
GPS	Global Positioning System
GTDS	Goddard Trajectory Determination System
Hi-CLASS	High Performance CO_2 Laser Radar
IOD	Initial Orbit Determination
LEO	Low Earth Orbiting
LS	Batch Least Squares
MSSS	Maui Space Surveillance Site
ODTK	Orbital Determination Tool Kit
SM-3	Standard Missile number 3
SP	Sequential Processing
STK	Satellite Tool Kit
RIC	Radial, In-track & Cross tack
RMS	Root Mean Square
RV	Reentry Vehicle

THIS PAGE INTENTIONALLY LEFT BLANK

ACKNOWLEDGMENTS

First and foremost, I would like to say “mahalo nui loa” to Professor Kyle T. Alfriend. Your ability to take a complex topic and simplify it was second to none. You inspired and fostered my erudition. Thanks for the countless hours you spent getting me to understand this math intensive topic. I would also like to thank Dr. Tom Kelecy of Boeing and Paul Black of Analytical Graphics Inc (AGI), whose help with the Orbital Determination Tool Kit (ODTK) program made the results herein possible. Dr. Chris Sabol was also a great help in the framing of the problem and giving guidance where needed. I would like to thank Professor Danielson for his help in the wording and flow of the thesis. I would also like to thank AGI for allowing me to use their Satellite Tool Kit and ODTK software.

On a personal note, I would like to thank the “boys” in the Guidance Navigation and Control Lab. Doctors “to be” Ryan Lewis and Kevin Bollino and Dr. Pooya Sekhavat were my day-to-day saviors when problems arose and they tolerated my outbursts and frustration. A special thank you should go to Ryan Lewis, without whose tutelage I would have had a much more difficult time completing this degree and thesis. Thank you to my children, Josephine, Gabrielle and Sophia, who afforded me the time to complete this degree and thesis while missing ballet recitals, martial arts practices, birthdays and myriad other fatherly responsibilities. Finally, THANK YOU to my wife, Amy, whose steadfast support throughout my career made me strive toward this degree and whose dogmatic review of my sixth grade writing style makes me sound intelligent. I share this degree with you.

This thesis is the culmination of two and a half years of my life and with input from many faculty and staff at Naval Postgraduate School. While they may be un-named herein, many faculty members provided valuable insight in their day-to-day teaching and direction along the way. Thank you.

THIS PAGE INTENTIONALLY LEFT BLANK

I. INTRODUCTION

This thesis investigated and compared the accuracy the estimation of a ballistic missile trajectory using four types of measurements: range-only; range, azimuth and elevation; azimuth and elevation; as well as range and range rate. Sensor measurements are commensurate with current values of telescopes and laser ranging devices. Further investigated was the use of two sites vs. a single site as well as the usefulness of observations from 30° above ascending visual horizon to 30° above descending visual horizon observations (30° - 30°) as well as 30° above ascending visual horizon to maximum elevation above ascending visual horizon observations (30° – 90°) for both types of sites. Waiting to determine the orbit until the 30° downward trajectory is less than ideal because at the time of the last observation, the object has almost impacted its intended target.

A. MISSILE TRACKING BACKGROUND

The United States currently employs many systems to affect ballistic missile defense. These systems predominantly include radars that are either S-Band or X-Band. These assets are either mobile or fixed. Fixed sights include those update early warning radars which are forward deployed as well as located near or within the United States. These radars can track in bound objects on ballistic trajectories primarily from the cued acquisition mode. That is to say they require a reasonable estimate of a missile position prior to being able to effectively track and lock the object. The sources rely upon intelligence and analysis of potential threat launch areas to “look” in the general direction in the sky. A portion of mobile platforms also exist that use SPY-1 radars which are located on all U.S. Navy combatant class ships and the Observation Island class of ships which use a somewhat different x-band radar system. These systems can work in local autonomous mode and do not necessarily require the use of another asset to accurately determine the initial location of the missile. As long as the radar is in acquisition dwell, it does not have high fidelity and can

generally only execute sector searches. In this mode, the launch event can be identified, but in order to determine an accurate classification of the missile, the system needs to be switched to a longer dwell time.

A fundamental knowledge of these systems will better prepare the reader for the topic at hand. The AN/SPY-l radar system is the primary air and surface radar for the Aegis Combat System installed in the Ticonderoga (CG-47) class (shown in Figure 1) and Arleigh Burke (DDG-51)-class warships. It is a multi-function phased-array radar capable of search, automatic detection, transition to track, tracking of air and surface targets, and missile engagement support.

Figure 1: USS Lake Erie (CG-70) a Ticonderoga class guided missile cruiser

A conventional, mechanically-rotating radar, "sees" a target when the radar beam strikes that target once during each 360° rotation of the antenna. A separate tracking radar would be required to engage each target. In contrast, the

computer-controlled SPY-1 Phased Array Radar of the AEGIS system (aptly named after the mythological shield of Zeus) brings these functions together within one system. The four fixed arrays of SPY send out beams of electromagnetic energy in all directions simultaneously. This continuously provides a search and tracking capability for hundreds of targets simultaneously. AEGIS as a part of the Theater Ballistic Missile Defense (BMD) in combination with the SM-3 intercept missile has been successfully used to track and intercept targets on ballistic trajectories.

The SPY-1 radar works exceptionally well and has been very effective for tracking space-based objects or objects on ballistic re-entry. A minor problem with the radar is that the system is designed for blue water and littoral operations. Consequently, the SPY-1 configuration must be modified to look above the terrain to avoid causing excessive false targets from land clutter. These configuration changes may increase ship susceptibility to low and fast targets. This makes it a less than ideal system to use near land for tracking objects that come over the landside horizon. Additionally, the DDG-51 Class are not equipped with a secondary air search radar which could leave some ships open to potential threats.

Additional limitations are with respect to handoffs and engagement tactics. In order to engage a target, the radar must hold a SPY-1 track. It cannot engage on a remote or otherwise handed off track unless equipped with special features such as the “Cooperative Engagement Capability.”

The missiles that are tracked generally contain single, but some times multiple, boosters or stages. The sample missile pictured in Figure 2 would have one or more separable phases to boost the warhead into space. After separation, these engines would fall away leaving only the warhead on a ballistic reentry. This indicates that with no other forces acting upon it other than the atmosphere, the missile would fall to earth in a predicable manner. This is when the intercept can be most accurately planned. For a short time, the warhead will fall as a single object, but after a period of time, some warheads separate into

multiple warheads scattering their potential impact over a significant area. Each of these multiple warheads fall and separate differently. Some weapons contain dummy warheads mixed in with the live warheads to potentially confuse targeting systems. This thesis considers only a single warhead.

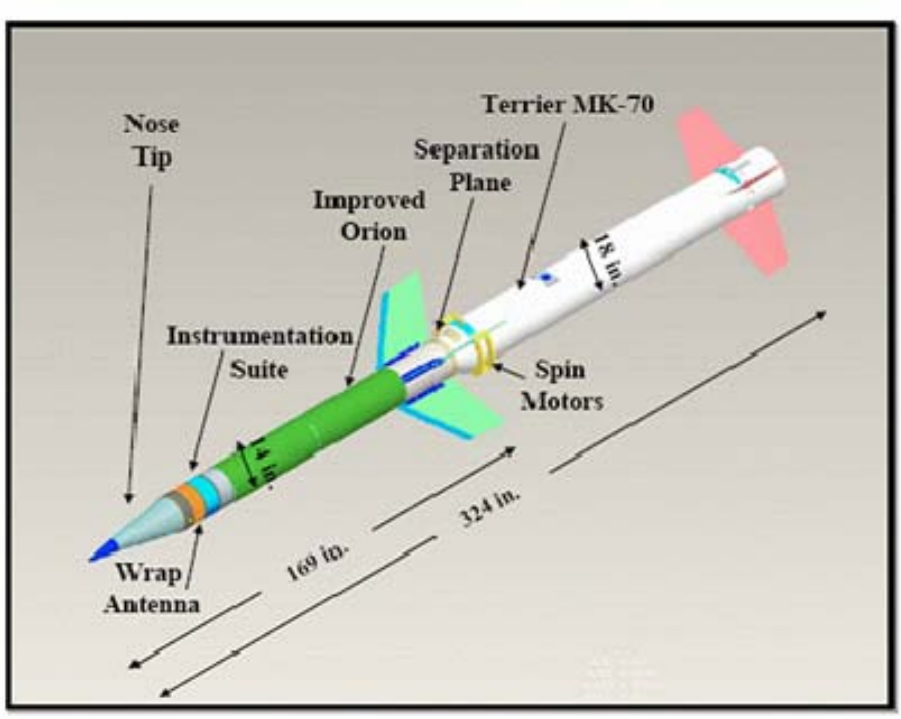

Figure 2: Sample missile

B. PURPOSE OF THIS THESIS

Angles measurements from optical systems are the primary source of data for maintaining the orbits of high altitude satellites. When determining the orbit from a single pass the performance of angles-only data is not as good as radar systems due to the lack of range data; however, if combined with laser ranging observations become particularly useful. Based on the concept that a ballistic trajectory is nothing more than a highly elliptical orbit whose perigee happens to intersect the earth, the same primary source for orbit determination for high altitude satellites can be applied to the highly elliptical Low Earth Orbiting (LEO) case. Recently it has been shown that the accuracy of the orbit updates using optical system angles-only data is just as good, if not better, than the

performance from radar systems for LEO satellites.[1] Other recent work has shown that the relative motion of satellites can be determined using differential angles data, that is given the motion of one satellite (the primary) the motion of a neighboring satellite relative to the primary can be determined using the differential angle data.[2] The purpose of this thesis is to investigate the use of angles data in determining the trajectory of a single missile.

This thesis uses Analytical Graphics' Satellite Tool Kit (STK) and Orbital Determination Tool Kit (ODTK) to generate sample trajectories and simulate observations range, range rate, azimuth and elevation and then from these observations estimate the missile trajectory. ODTK will be further described in the next section. Both tools are invaluable resources because they allow the users to perform multiple scenarios given different starting and stopping points without actually expending the required cost on launching missiles.

High Performance CO_2 Laser Radar (Hi-CLASS) is a CO_2 laser at the Maui Space Surveillance Site (MSSS) which can work in conjunction with the Advanced Electro-Optical System (AEOS) passive sensor. Hi-CLASS uses the laser to image satellites. The Hi-CLASS has object metric measurement accuracies of range resolution two meters, velocity resolution one meter per second and angular resolution eight microradians. These resolutions were used to display worst-case ability of this site to track a missile.

While the MSSS sensors have merit for determining orbits given the assumed trajectories, it is not meant as a substitute for the already in place BMD system. The Maui system is superb for analyzing trajectories that pass near overhead of the observatory. The further the trajectory away from the site, the less effective the visual and laser ranging becomes. Given the fact that there are no "threat" trajectories that pass over the MSSS sight, these sensors and this

[1] M.L. Thrall, *Orbit Determination of Highly Eccentric Orbits Using a Raven Telescope*, Master's Thesis, Naval Post Graduate School, Monterey, California, September 2005

[2] K.C. Hill, C. Sabol, C. McLaughlin, K.K. Luu, and M. Murai, "Relative Orbit Determination of Geosynchronous Satellites Using the COWPOKE Equations," Paper No. AAS 04-195, AAS/AIAA Space Flight Mechanics Conference, Maui, HI, Feb. 2004.

concept are not intended to substitute for the existing BMD systems. This thesis demonstrates the value of angle data in aiding missile trajectory estimation.

Also considered was the use of an additional sensor in the form of an AEGIS ship near the coast of the launch point to track longer and hand off a missile given moderate sensors. The AEGIS system has assumed object metric measurement accuracies of range resolution five meters and angular resolution 540 microradians. These resolutions were used to display worst-case ability of this site to track the missile.

Chapter II outlines orbit determination background, types and methods. Chapter III describes the inputs to ODTK as well as STK such that the results can be reproduced. Chapter IV discusses the results using a single and multiple sites. Chapter V describes the conclusions and Chapter VI suggests possible future work.

II. ORBIT DETERMINATION

A. ORBIT DETERMINATION BACKGROUND

Orbit prediction is the calculation of the orbit of an object given the state, the position and velocity or orbital elements, at some time (epoch). Orbit determination is determining the state at the epoch from a set of observations. Since the observations are spread over time, the orbit must be predicted from one observation time to the next. Thus, orbit determination requires an orbit prediction model. Orbit determination began around 1610 with Kepler. Others, such as Legendre and Gauss, have continued the work, giving the science a firm analytical and computation basis. Many improvements in theories have been cultivated over the years, but the fundamentals remain the same.

Gauss's theory is not used today because ultimately, the data that was gathered at the time lacked credible observations and present day theories expand upon the original theory making it less useful. Without improvements in observational instruments, many of the techniques used in the 19th century for planets and comets would be useless for satellites. For instance, if Gauss had been attempting to estimate the orbit of a much closer object such as a LEO satellite, he would probably have been frustrated because his results would not have been consistent enough to publish. The observations techniques of the era would not have been accurate enough to support his calculations.[3]

An important discovery in estimation techniques came about in the early 1900 when Sir Ronald A. Fisher (1890-1963) introduced the concept of the "*maximum likelihood method.*" This work extended Gauss's least squares method to cover non-Gaussian error statistics. This independent approach seemed to begin the next advancement in estimation techniques.

Another major event occurred in 1958 when Peter Swerling (1929-2000) published a RAND corporation report discussing a recursive algorithm for

[3] David A. Vallado, *Fundamentals of Astrodynamics and Applications*, 2nd Edition, p. 675, Microcosm Press, 2004

statistical orbit determination. Others seemed to simultaneously discover similar methods. This small industry seems to be beset with simultaneous discoveries such as Gauss and Legendre in the early 1800s. Contention surrounds the publication of Rudolf E. Kalman's (1930) landmark work titled, "*A New Approach to Linear Filtering and Prediction Problems*." Many researchers have attempted to improve the initial concepts of Kalman, and have made minor advances, but the method remains in Kalman's name. In all fairness, these "newer" recursive formulations are a variation of the original contributions of Gauss and Legendre.[4]

The United States' first modern event in determining orbits came when Sputnik I flew overhead. This seemed to mark the beginning of the modern discipline of orbit determination. The methods were steeped in traditional astronomy, but differed in three essential ways. First, typically satellites were tracked via radiometric techniques, rather than via telescopes. The second focus was on Earth-centered orbits, rather than orbits around the sun or distant planets. Third, there was reliance upon intensive numerical calculations, rather than estimates and heuristics.

The science progressed quickly in its formative years, thanks to the rapid advances in computing technology that accompanied the early space race. Such developments made it possible to solve the mathematics that govern the orbital motion equations in a reasonable time. Much of the early work focused on generating better timetables of satellite speed and trajectory. Large computers would calculate the complex equations of motion to generate these tables, and the results would be compared with actual radio measurements from tracking stations.[5]

B. INITIAL ORBIT DETERMINATION

There are two types of orbit determination. First is an Initial Orbit Determination (IOD). While an IOD for distant objects can be made with a simple

[4] David A. Vallado, *Fundamentals of Astrodynamics and Applications*, 2nd Edition, pp 676, Microcosm Press, 2004

[5] http://www.aero.org/publications/crosslink/summer2002/04.html, Mar 06 Accessed Nov 06

linear problem resulting in explicit solutions, IOD for near earth objects is considerably more difficult. ODTK includes a Herrick-Gibbs algorithm to calculate an initial orbit from range and angle measurements and a Gooding algorithm to calculate an initial orbit from angles-only measurements. Albeit ODTK uses a navigation solution algorithm to calculate an initial orbit from GPS pseudo ranges, this was found to be insufficient for obtaining range-only or range and range rate IODs that converge in the allotted time span for a missile trajectory because of the required closeness in observations for the IOD. Since no adequate IOD was available that would accommodate the given missile trajectory time frame, the range-only and range and range rate scenarios incorporated a manually modified range, azimuth and elevation Herrick-Gibbs IOD that was biased to be less accurate than the normal range, azimuth and elevation IOD. Since the IOD used is accurate, it is understood the range-only and range and range rate simulations may be optimistic.

Herrick-Gibbs is an algorithm named after the authors that obtains an estimate of the velocity at the time of the middle observation given three sequential position vectors and their observed times. Herrick-Gibbs is a variation of the Gibbs method and employs a Taylor series expansion to obtain an expression for the middle velocity vector. The closer the position vectors are in time, the greater the impact of observational errors on the final result.[6] Similarly, Gooding angles-only theory estimates the position and velocity of a spacecraft from three pairs of angles measurements and its tracking platform position. The tracking station selected is currently fixed, but this theory has practical application if applied to a moving tracking station, such as a satellite, as long as the exact position is well known.

C. STATISTICAL ORBIT DETERMINATION

The second type of orbit determination is an orbit update. This assumes an ephemeris already exists, such as from an IOD or previous orbit

[6] David A. Vallado, *Fundamentals of Astrodynamics and Applications*, 2nd Edition, pp 441-442, Microcosm Press, 2004

determination, and as the name implies, the ephemeris is updated using new observations. In terms of obtaining a better orbit for a satellite, the traditional orbit update is not useful for the purposes of this thesis because, as seems evident, there will be no "next time" the missile passes overhead to formulate a better solution. However, the orbit can be updated in near real time using the IOD and this is what ODTK does.

1. Least Squares

The batch Least Squares (LS) method processes successive batches of data. LS methods input tracking measurements with tracking platform locations and an a priori orbit estimate and output a refined orbit estimate and the covariance. An a priori orbit estimate is required. An a priori covariance can be used, but is not required. Associated output error magnitudes are small when compared to IOD outputs. LS methods consist of a sequence of linear LS corrections, where sequence convergence is defined as a function of tracking measurement residual Root Mean Square (RMS). Each linear LS correction is characterized by a minimization of the sum of squares of the tracking measurement residuals. LS methods produce refined orbit estimates in a batch mode, together with error covariance matrices that are optimistic; i.e., orbit element error variances are typically too small, often by at least an order of magnitude. This is due to the fact that the LS method assumes a perfect dynamic model. Operationally, LS may be the only method used, or it may be used to initialize Sequential Processing (SP). LS algorithms require elaborate software mechanisms for measurement editing. ODTK uses the accurate QR factorization and triangularization method with orthogonal Householder transformations to solve the LS equation.[7]

The LS method also provides a statistical confidence in the uncertainty of the answers, the covariance. The covariance matrix contains the estimates for the closeness of the fit with the chosen dynamics. Given the state

[7] OD Tool Kit: A Technical Summary, 4th edition, v.3, p. 9, 2004

$\mathbf{x} = (x_1, x_2, \ldots, x_n)^T$ the covariance is of the form in Equation (1) where σ_{x_j} is the standard deviation of x_j and μ_{jk} is the correlation coefficient of x_j and x_k.

$$P_{\mathbf{xx}} = \begin{bmatrix} \sigma_{x_1}^2 & \mu_{12}\sigma_{x_1}\sigma_{x_2} & \cdots & \mu_{1n}\sigma_{x_1}\sigma_{x_n} \\ \mu_{12}\sigma_{x_1}\sigma_{x_2} & \sigma_{x_2}^2 & \cdots & \mu_{1n}\sigma_{x_2}\sigma_{x_n} \\ \vdots & \vdots & \ddots & \vdots \\ \mu_{1n}\sigma_{x_1}\sigma_{x_n} & \mu_{1n}\sigma_{x_2}\sigma_{x_n} & \cdots & \sigma_{x_n}^2 \end{bmatrix} \quad (1)$$

2. Kalman Filter

The Kalman Filter is one of the most useful estimation tools available today. Loosely speaking, Kalman filtering provides a recursive method of estimating the state of a dynamical system in the presence of dynamic and measurement noise. A key feature is that it simultaneously maintains estimates of both the state vector ($\hat{x}$) and the estimate error covariance matrix (P). This is equivalent to implying the output of a Kalman filter has a Gaussian probability density function with a mean $\hat{x}$ and a covariance *P*.[8] The Kalman filter is a tool for linear systems. The orbit equations are highly nonlinear. The Extended Kalman filter (EKF) is the application of the Kalman filter to nonlinear systems in which the system equations are linearized about the reference trajectory. The EKF is a powerful tool when the system is modeled correctly and the deviations from the reference trajectory are small enough to be represented by a linear system. This is analogous to the use of least squares and the linearization about the reference trajectory.

While the exact algorithm is proprietary, ODTK employs a Kalman filter. The current terminology is optimal sequential filter. ODTK's filter is a forward-time recursive algorithm consisting of a repeating pattern of filter time updates of the state estimate, which propagates the state estimate forward, and filter measurement update of the state estimate which incorporates the next measurement. The filter uses the observations along with their location and a

[8] Lynch Choset, Kantor Hutchinson, Kavraki Brugrard and Thrun, P*rinciples of Robot Motion,* p. 269, MIT Press 2005

priori state estimate as the input, and provides optimal state estimates and realistic state error covariance matrices as the output, updated after every observation and at 1-second intervals[9].

AGI's ODTK was used for processing and simulating observations and determining the orbit. The program was responsible for all the data processing. Testing of the software was completed to ensure comparable results from separate approaches before serious attention could be used on the results. The ODTK output was compared against the industry-standard Goddard Trajectory Determination System (GTDS) [10]program's output as well as output from Dr. K.T. Alfriend's numerical model assuming an elliptic orbit about a non-rotating Earth. All outputs have similar outcomes thereby providing triple verification of the results.

D. ERROR ESTIMATES

For the purposes of this thesis, the covariance provides information on the accuracy of the orbit determination. It can be used for comparison or just for a single fit. For the covariance to provide a valid assessment of the orbit determination accuracy, the dynamics and sensor errors have to be accurately modeled. If one is comparing covariances, one can reasonably argue in some cases if both are in error in the same manner, the comparison is valid. For example, if the actual measurement errors for both fit spans are five arc-seconds, but are modeled as 10 arc-seconds, then the comparison should be valid.

The initial covariance is input as "orbit uncertainty," listed in the satellites settings. It is input in the Radial, In-track & Cross track (RIC) reference frame. The initial covariance requirements for all sets of data should be representative of the actual uncertainty based on the types of measurements and the IOD. For instance, the Herrick-Gibbs would give a good position estimate, but the velocity

[9] ST/ODTK Manual, Analytical Graphics Inc., February 2006

[10] Computer Sciences Corporation and NASA/GSFC Systems Development and Analysis Branch (Editors), *Research and Development Goddard Trajectory Determination System (R&D GTDS) User's Guide*, July 1978.

is not well known. The Gooding angles-only should give a good in-track and cross-track position estimate, but the radial will be poor. “Range-only” yields a good range estimate which is a combination of radial and in-track, but the cross-track will be poor as well as the velocity. “Range rate” will be much like range but in addition, there will be a reasonable velocity estimate along the line of sight, which is a combination of radial and in-track. Since significant analysis would be required to determine the initial covariance for the IOD methods, an initial covariance was not accomplished.

White noise is added to each sensor from the facility commensurate with the fidelity of the sensor selected. The fidelity is defined as the standard deviation of the sensor. This ensures the accuracy of the scenarios. As seems evident, the more accurate the sensors, the less the error.

THIS PAGE INTENTIONALLY LEFT BLANK

III. ODTK & STK INPUTS

STK is used to generate the original trajectory from lift off point to destination assuming a best-fit ballistic trajectory as shown in Figure 3. For the purposes of this study, the trajectory path was limited to those which flew from Vandenberg Air Force Base to Kwajalein Atoll. The trajectories are optimal predicated upon drawing a straight line through two points, the take off and the touchdown on a sphere, and using a plane propagated outward from the line to generate. The ballistic trajectory has as input the start location and time, maximum altitude as well as stopping location. For optimal trajectory, altitude input is zero and STK generates an optimal trajectory. The trajectory data is exported to ODTK and an initial state of the missile at the launch time is generated using the initial state tool. The exact scenario settings for ODTK are found in Appendix A.

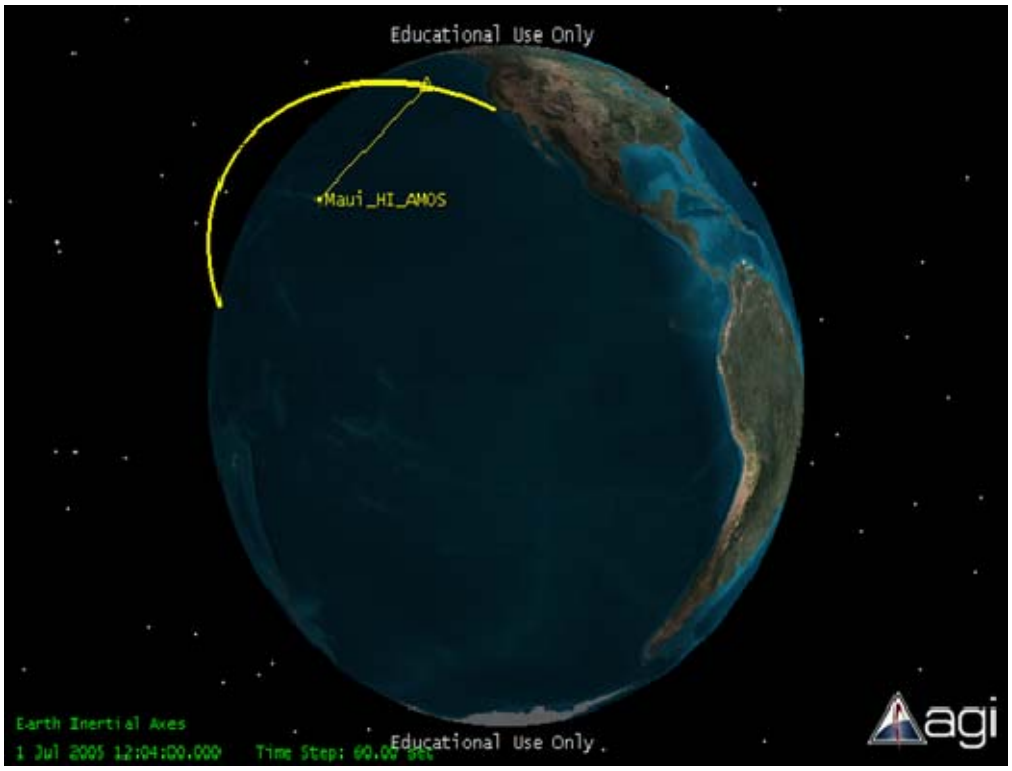

Figure 3: STK visual of ballistic arc

Using the initial state, a truth trajectory is generated using the simulator options. The MSSS at Haleakala is manually entered into the scenario using the exact latitude, longitude and altitude. Simulated observations of range, azimuth, elevation and range rate for the exact flight path trajectory as seen from the facility are generated. Then white noise with a standard deviation of the input measurement noise is added to the truth observations. These noisy observations are the observations used for the trajectory estimation. The ODTK sequential estimator needs an initial state estimate and initial covariance. These will obviously be different according to the set of observations being used. As discussed in the Initial Orbit Determination chapter, there are options in ODTK for angles-only and range and angles measurements. Both of these methods require three observations. Choosing observations evenly spaced and spanning the entire trajectory would allow the most accurate orbit determination, but would preclude obtaining the orbit until shortly after the last observation occurs. In the case of orbit determination for a missile, waiting has reduced efficacy because at the time of the last observation, the object has almost impacted its intended target. A compromise was identified to select a range of initial observations with a narrow spread to obtain an orbit in the timeliest manner while allowing a sufficient spread between the observations to determine the orbit with minimal error. For this thesis the first, third and fifth observations (approximately a 40 second spread) are selected and an initial orbit is determined. Exact inputs to the Initial IOD are detailed in Table 1.

Table 1: Selected Measurements for IOD from Maui site.

Seconds since start	Date	Time	Range (m)	Elevation (°)
0000	01 Jul 2005	12:08.20.00	2057.878	31.176
0020	01 Jul 2005	12:08:40.00	2013.291	33.592
0040	01 Jul 2005	12:09:00.00	1971.066	36.037

The user can select options for IOD when using ODTK. Herrick-Gibbs algorithm can be used to calculate an initial orbit from range and angle measurements; a Gooding algorithm can be used to calculate an initial orbit from

angles-only measurements, and a navigation solution algorithm to calculate an initial orbit from Global Positioning System (GPS) pseudo ranges. Once the initial orbit is determined, an initial state vector is formed for the missile starting at the time determined by the IOD method. The Herrick-Gibbs was used to generate an IOD for this all scenarios with modifications as stated in the Initial Orbit Determination section. Since the Herrick-Gibbs algorithm was selected, the IOD object starts the epoch using the middle time from the three selected initial measurements.

The filter is run with the error missile state that contains the built in sensor errors which yields an uncertainty "cone" as seen in Figure 4. This cone represents the outside boundaries of the possible actual trajectories given the errors and biases encountered. The resulting expanded predicted "known" position of the missile forms a cone of uncertainty. Ephemeris data was exported from ODTK and loaded into STK to generate a visual representation of the error ellipsoid (Figure 5) for each determined position. Great caution is required to ensure the filter, simulator, missile, initial orbit determination and facility blocks have the same sensors selected.

Once the filter run is completed and the filter and simulator runs are differenced, the static product builder is used to select the desired output. Again, great care must be taken during this phase to ensure the correct input files are used to gather the specified output. The graphical representations are saved as bitmaps and the tabular results are exported into Excel files where the data can be easily manipulated. The outputs are formatted easily and modified by editing the output file type to gain the desired file type.

Scenarios using simulating observations of range, azimuth and elevation, angle-only, range-only, and range and range rate from the Maui site from the ground station to the target were first generated for the 30°-30° and the 30°-90° elevation passes. Each scenario was compared to the truth trajectory (the simulator ephemeras data) and the differences noted. The differenced trajectories highlight the maximum difference given the stated sensor errors.

Following this complete scenario run, the same type scenario was run with an additional sensor. The second sensor was assumed to be a ship with AEGIS which is approximately 150 miles off the coast of California. Its purpose is early acquisition of a missile launch and to allow tracking and hand-off to the sensor on Maui. This will increase the amount of time that the missile is being tracked and should yield a better orbit determination and subsequent superior update. The other thought is that the increased time of sensor observation should improve the angles-only orbit determination and update.

The Aegis ship can relay raw data such as range and angles to the Maui site. The IOD for the Aegis ship is accomplished with Herrick-Gibbs in a similar fashion as described above for the Maui site. The same compromise was identified to select a range of initial observations with a narrow spread to obtain an orbit in the timeliest manner while allowing a sufficient spread between the observations to determine the orbit with minimal error. The Aegis ship continues generate a trajectory and track the missile from 30° above its horizon to the point where the missile is 30° above Maui's horizon. At this point, the state and covariance from Aegis are handed off to the Maui site. This initial orbit is predicated upon a predetermined white noise which coincides with common resolution of the sensors. Exact inputs to the IOD are detailed in Table 2..

Table 2: Selected measurements for IOD from AEGIS ship site.

Seconds since start	Date	Time	Range (m)	Elevation (°)
0000	01 Jul 2005	12:01:50.00	637.5576	30.855
0020	01 Jul 2005	12:02:10.00	648.377	40.740
0040	01 Jul 2005	12:02:30.00	629.866	51.038

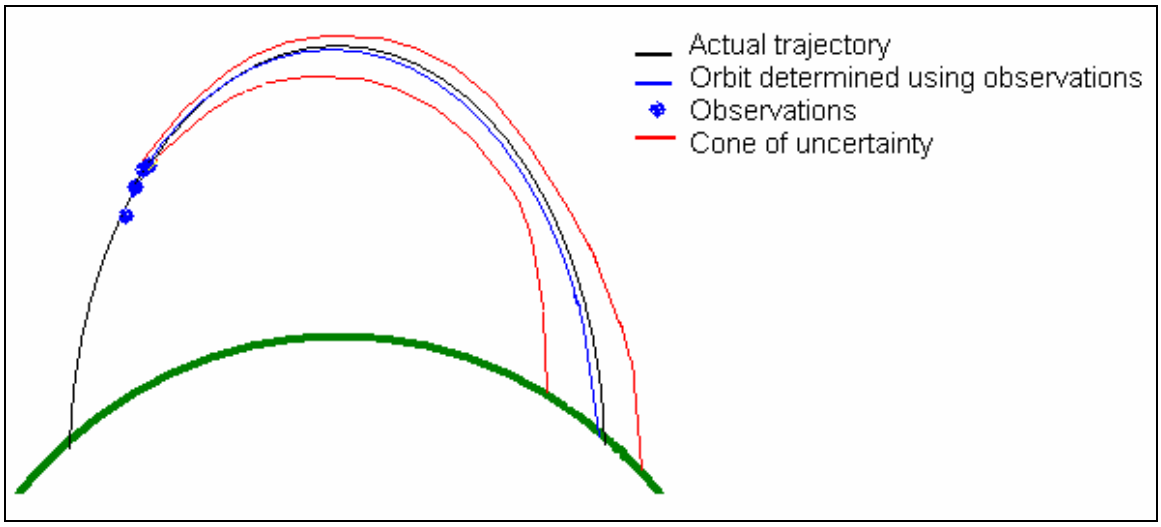

Figure 4: Cone of uncertainty

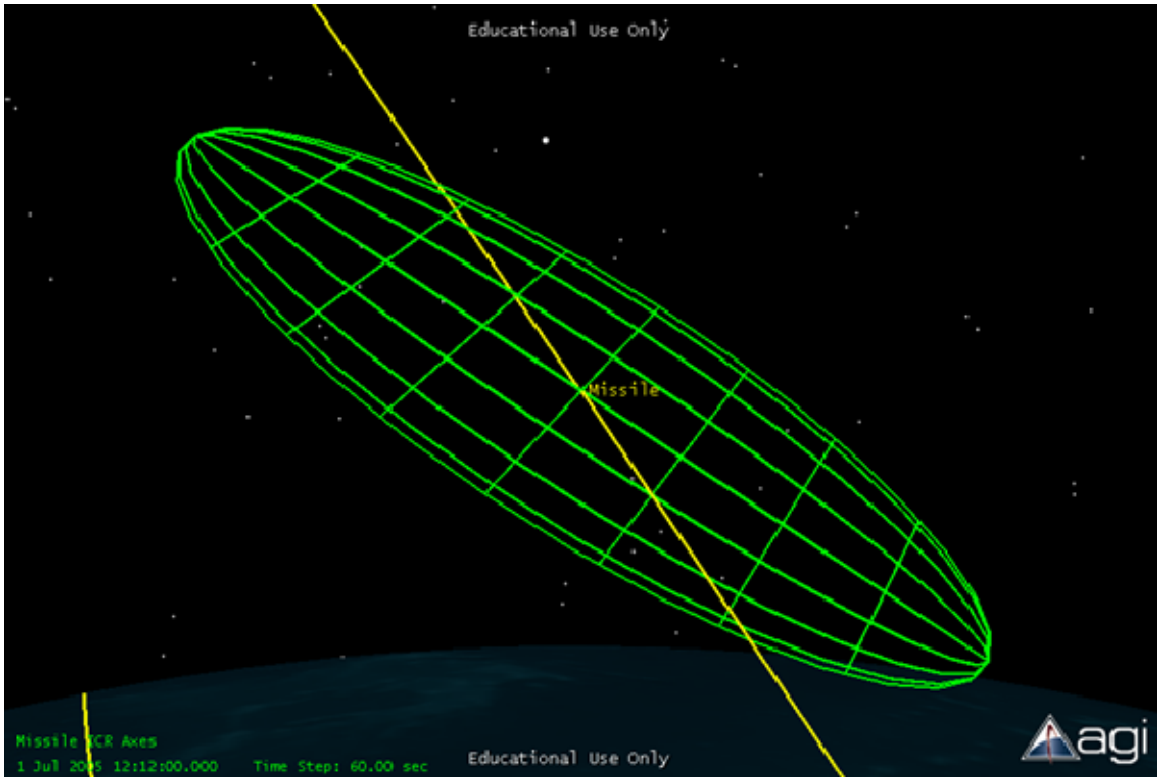

Figure 5: Error ellipsoid generated by STK

THIS PAGE INTENTIONALLY LEFT BLANK

IV. RESULTS

A. SINGLE SITE

The process described in the previous section was followed for creating simulated observations, calculating IODs and predicting the object's orbit from 30° above the horizon on ascent to 30° above the horizon on descent as well as 30° to 90°. The 30-30 solution is used to determine the trajectory of a fully tracked object and the 30-90 solution is to establish what would happen if an object was tracked until it was approximately overhead.

As discussed in the Orbit Determination section, the initial covariances should be representative of the initial position uncertainty. It is important that the initial covariance not be too small because this means that the initial position is well known and it may be difficult for the filter to converge on the correct solution and observations rejected. If it is too large then convergence takes too long or convergence may also be difficult. With a large number of observations the estimated state is somewhat independent of the initial covariance as long as it is not too small. Thus, there is a wide range of acceptable values for the initial covariance; it does not have to be precise, only representative. As discussed earlier the IOD methods do not provide a covariance and the amount of analysis to obtain the actual initial covariance would be significant. For the series of separate runs, the covariances in Table 3 were used. These values were a result of knowledge of the problem and some trial and error analysis.

Table 3: Initial Covariances for all Sigma

	σ_r	σ_i	σ_c	σ_{vr}	σ_{vi}	σ_{vc}
Range-Only	500 m	5 km	5 km	50 m/s	50 m/s	50 m/s
Range & Range Rate	500 m	5 km	5km	10 m/s	50 m/s	50 m/s
Azimuth & Elevation	50 km	1000 m	1000 m	50 m/s	50 m/s	50 m/s
Range Azimuth & Elevation	1000 m	1000 m	1000 m	50 m/s	50 m/s	50 m/s

1. Sensor Modeling

White noise is added to each measurement from the facility commensurate with the error indicated by the sensor. This ensures the scenarios are true to life reflections of the capabilities of the system. As seems evident, the more accurate the sensors, the better certainty the position of the object can be estimated. The stated sensor errors are; range resolution of two meters, velocity resolution of one meter/second, and an angular resolution of eight microradians. Full assumptions for measurement statistics are detailed in Table 4. Further assumed was the fact that the visual and laser sensors cannot "see" the object until it is 30° above the observation point's horizon. This limitation also extends to the ballistic and descending portion of the shortened trajectory.

Table 4: Measurement Statistics

	White noise sigma	Estimate Bias	Tropo Sigma	Light time delay	Count interval
Range	2 m	False	0	True	---
Range Rate / Doppler	1 m/s	False	---	True	1 sec
Azimuth	.000555556°	False	----	----	---
Elevation	.000555556°	False	.05	----	----

Light time delay setting is applicable to range and range rate only and allows ODTK to take into account the finite speed of light given the difference in time of the position of the object from the time light leaves the missile until the time the light arrives at the point of observation. The tropo sigma setting applies to range and elevation only and accounts for uncertainty in the tropospheric corrections. The count interval setting is applicable to the range rate only and specifies the length of the interval over which the Doppler count is generated. All measurements have some bias. With enough measurements the bias can be estimated. This analysis assumed a zero bias so the estimate bias setting was false.

To obtain the truth trajectory of the missile, the simulation is executed and a "simrun" file is generated using the truth initial state vector as input. Prior to the

filter run, the IOD is pushed onto the missile. This forces the filter to start its run from the position resulting from the IOD using the white noise indicated above, not the true position. The filter generates a “filrun” file. The filrun and simrun files contain ephemeris data for the trajectories and can be differenced. The resultant file is a “difrun” file and this diffrun contains the ephemeris data differences. The difrun file is used as input into the static product builder (a report generating feature of the ODTK software) and the Radial, In-track and Cross-track (RIC) positions were generated for each moment in time. For the purposes of time, the fidelity was stopped at every 10 seconds albeit the software has the ability to march times less than one second.

The standard deviations of the position uncertainty for RIC given each scenario are displayed in Figure 6 – Figure 11. The radial, in-track and cross-track uncertainties of the four measurement scenarios allow us to draw conclusions from a statistically significant number of runs instead of just from one simulation. Figure 12 - Figure 15 show the single case results that demonstrate the theory and these results coupled with Figure 6 – Figure 11 prove the foundation for the comparison of the four scenarios.

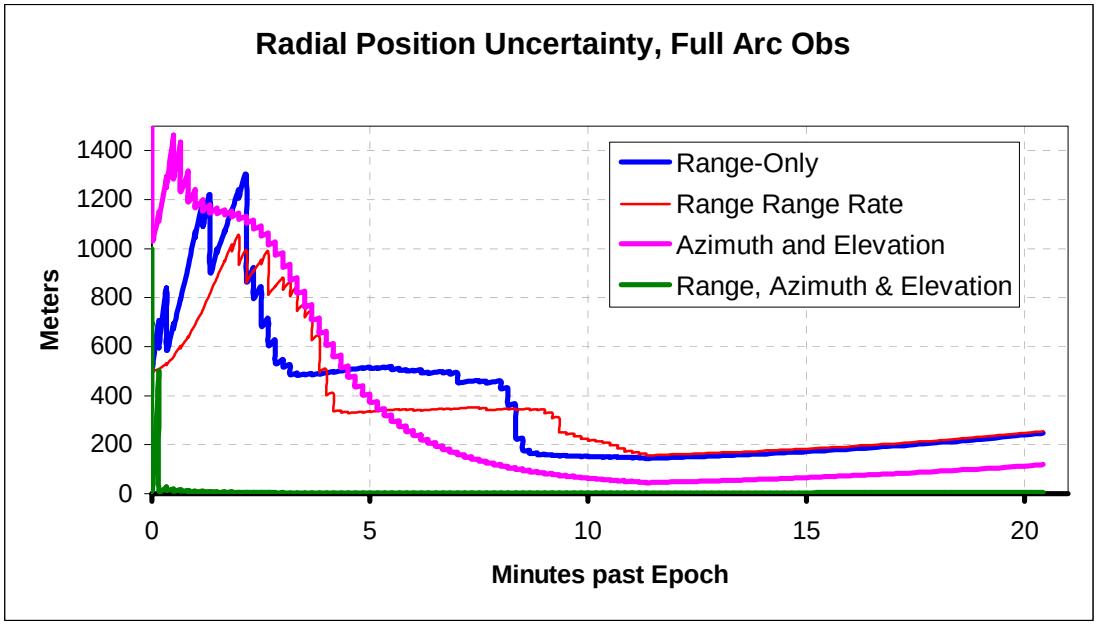

Figure 6: Radial Position Uncertainty, Full Arc Observations

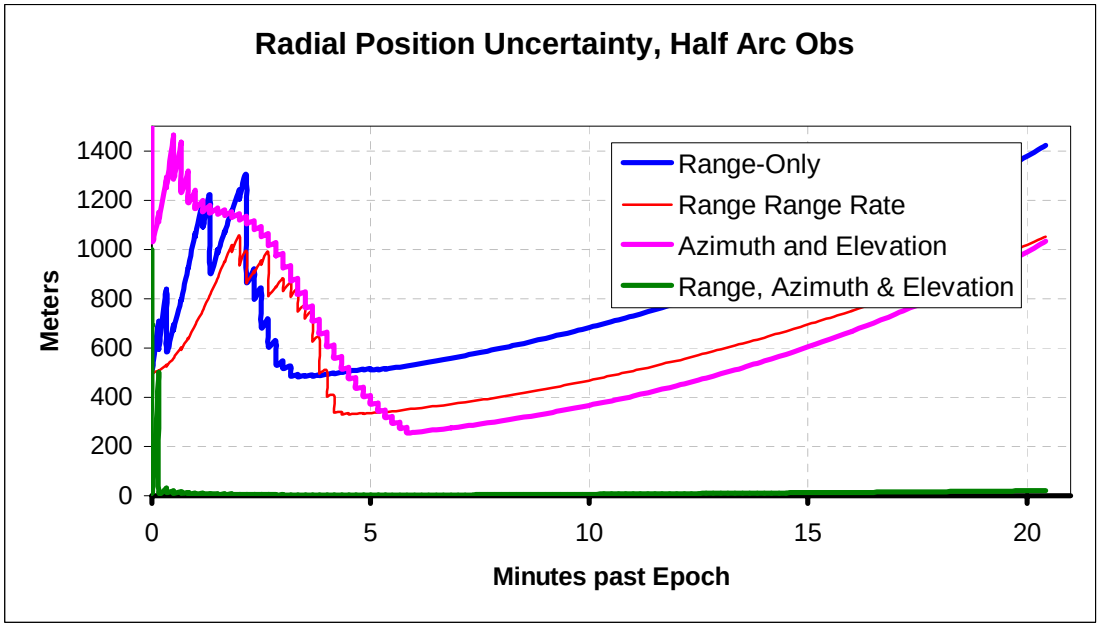

Figure 7: Radial Position Uncertainty, Half Arc Observations

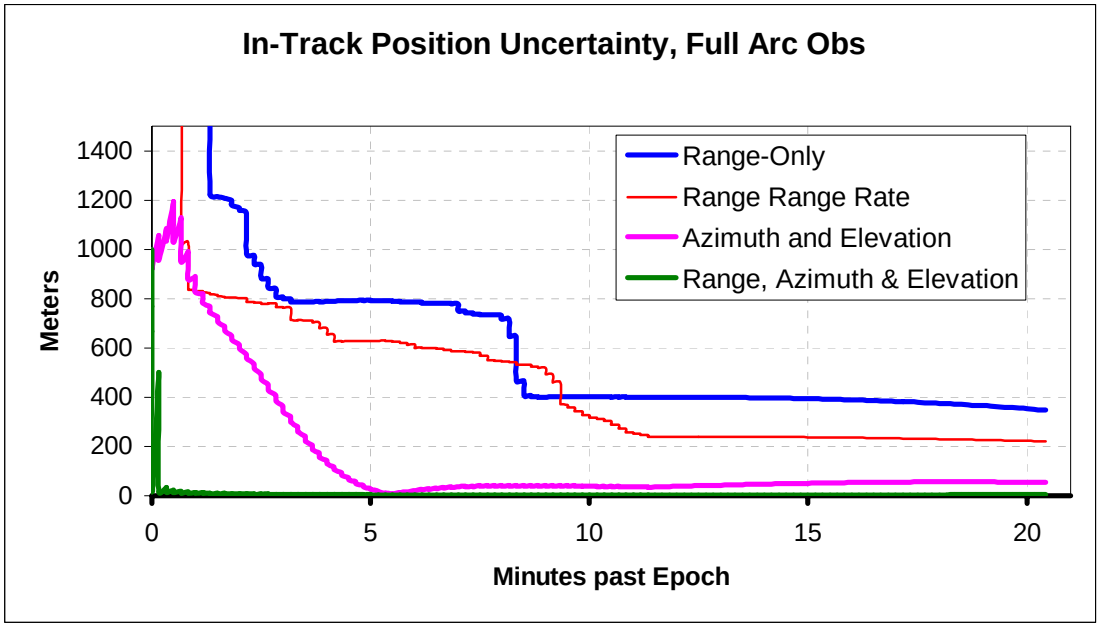

Figure 8: In-Track Position Uncertainty, Full Arc Observations

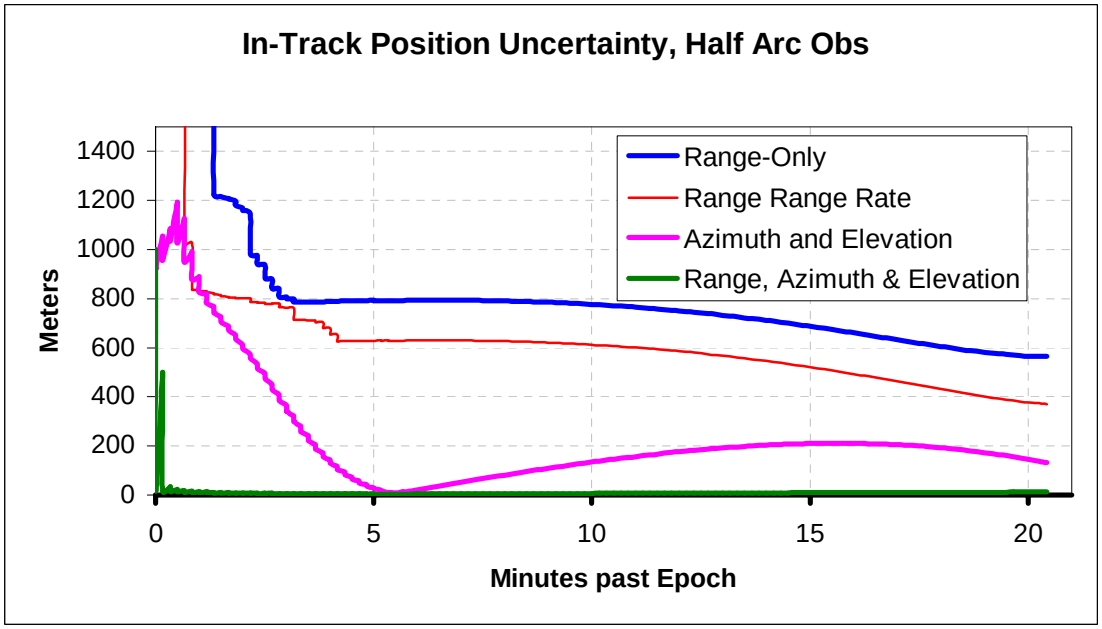

Figure 9: In-Track Position Uncertainty, Half Arc Observations

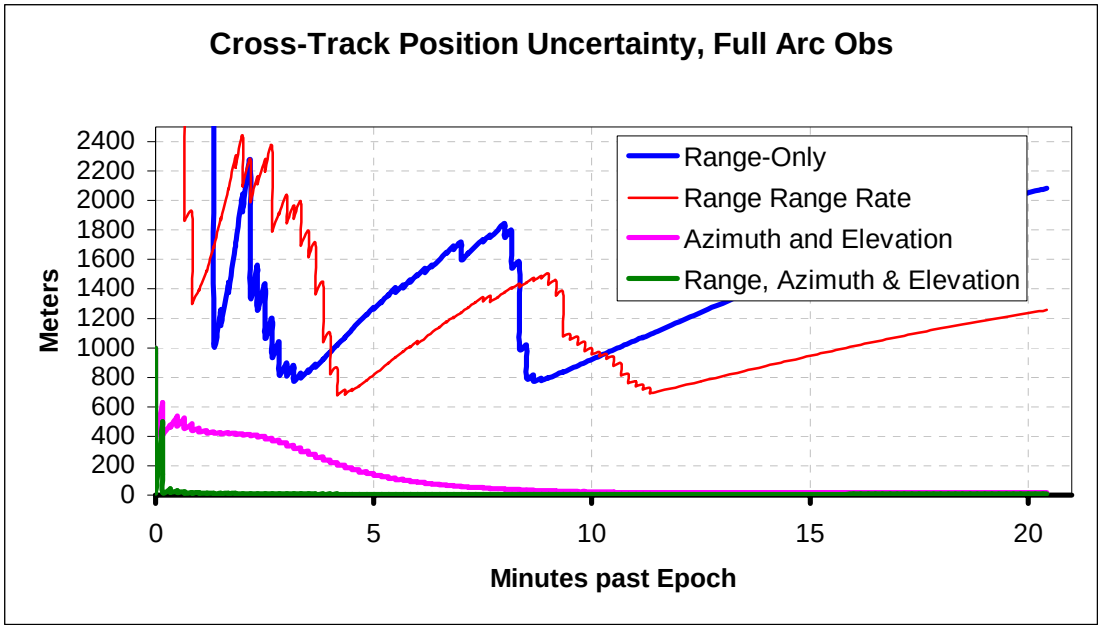

Figure 10: Cross-Track Position Uncertainty, Full Arc Observations

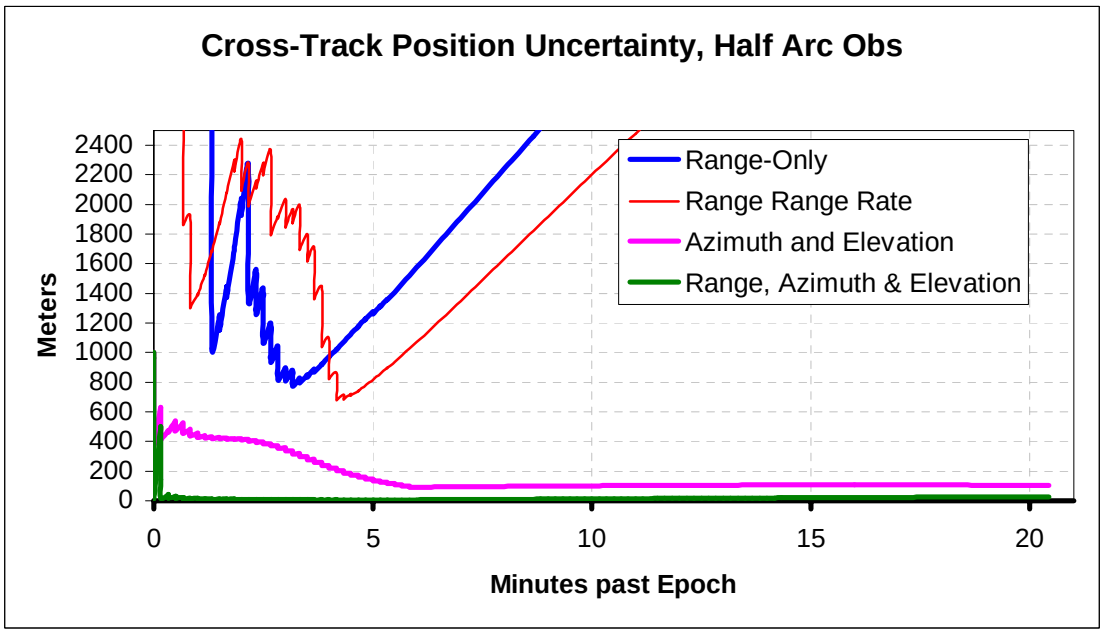

Figure 11: Cross-Track Position Uncertainty, Half Arc Observations

Details reports for the differenced radial position for each run are graphed in Figure 12 – Figure 15.

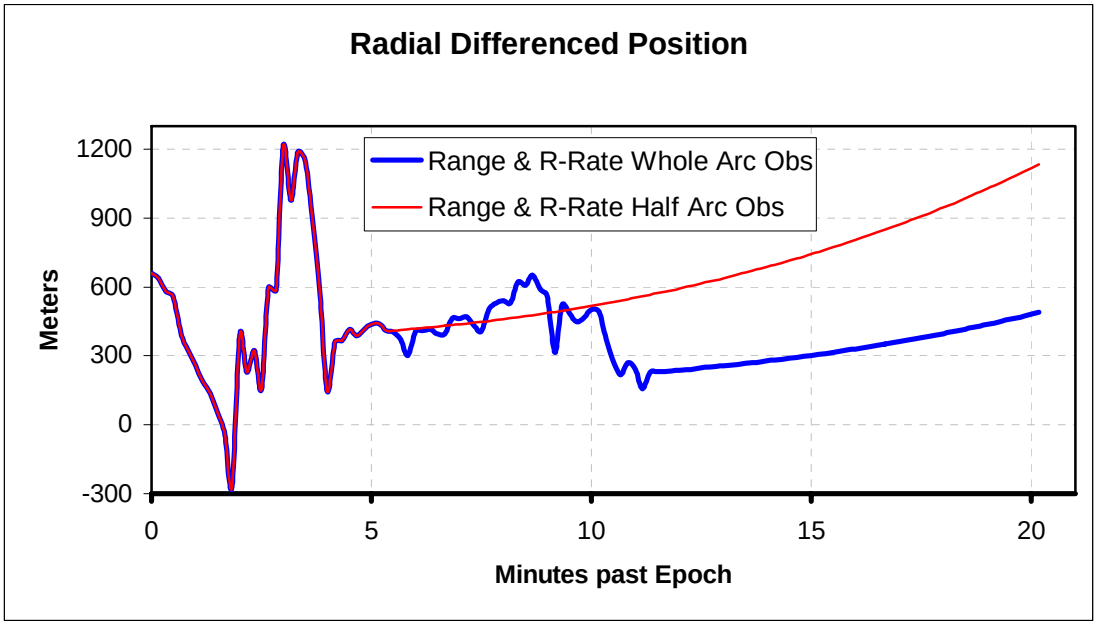

Figure 12: Differenced Radial Position for Range & Range Rate Observations

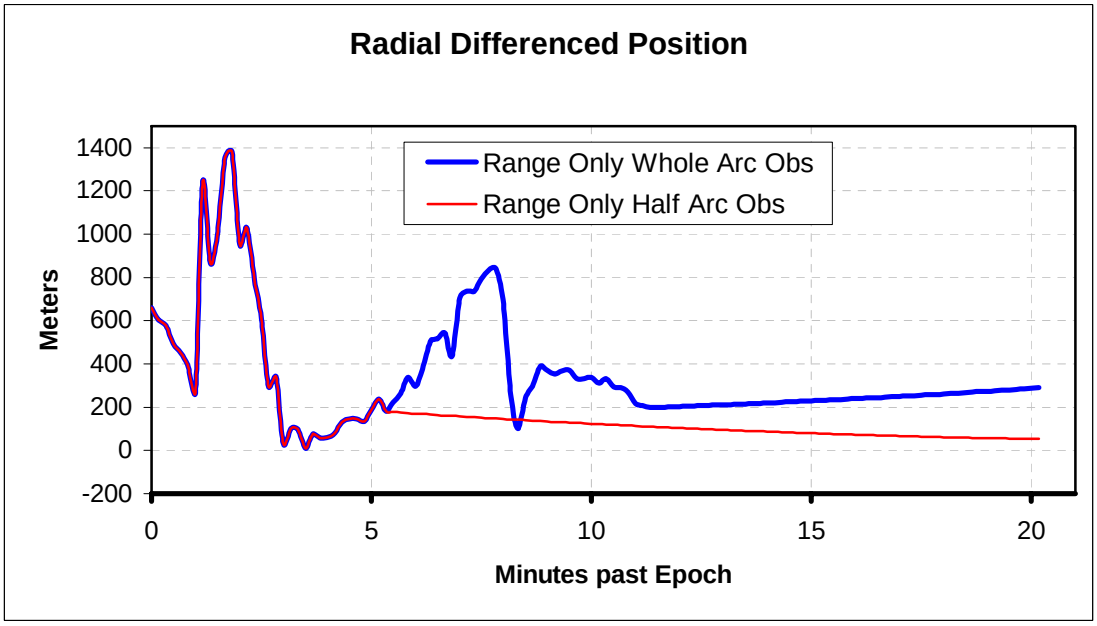

Figure 13: Differenced Radial Position for Range-Only Observations

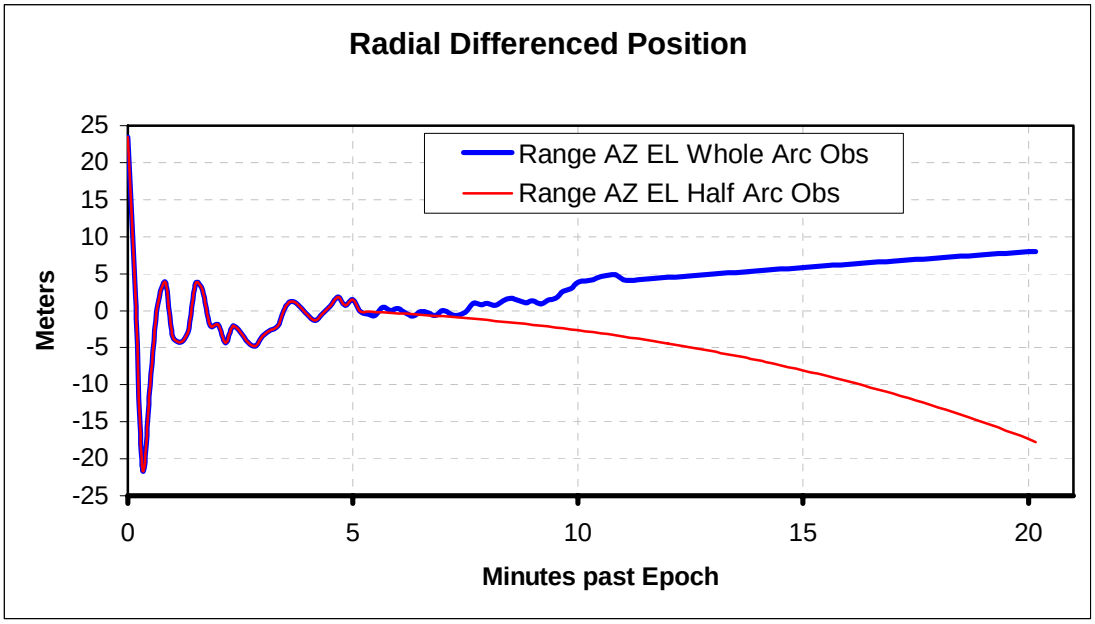

Figure 14: Differenced Radial Position for Range Azimuth & Elevation Observations

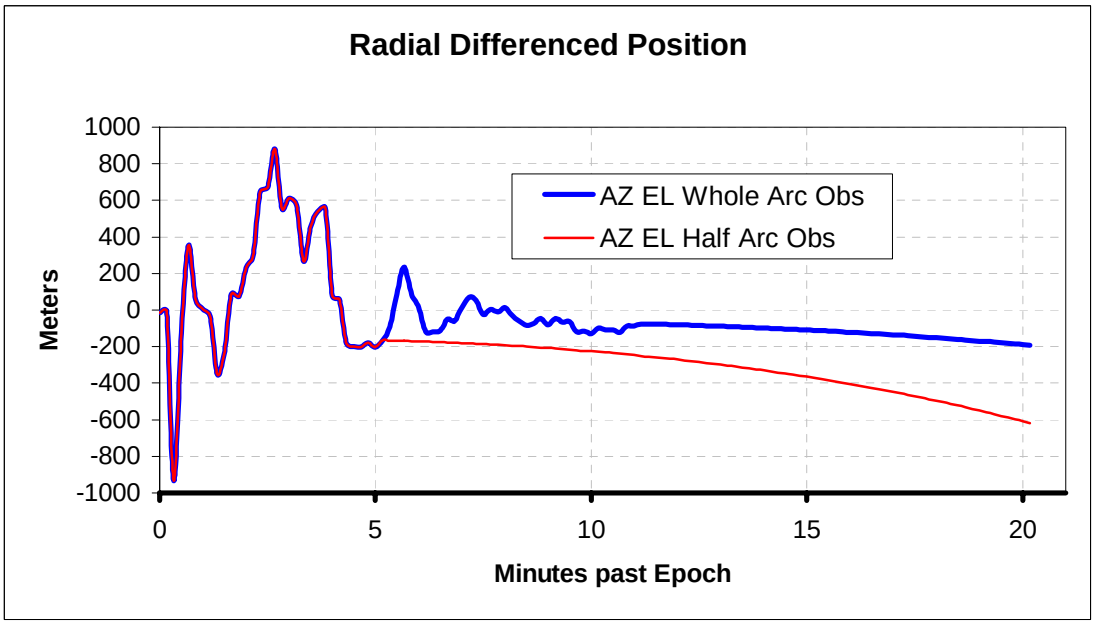

Figure 15: Differenced Radial Position for Azimuth & Elevation Observations

Epoch is the third time the sensor is able to “see” the object and start to simulate observations, which is in the center of the IOD observation span, the 3rd observation. Because the runs for both 30°-30° and 30°-90° are predicated upon the same data initially, their tracks overlay one another until the maximum elevation, which is where tracking in the 30°-90° scenario ends. This is 14.1667 minutes from initial launch and approximately six minutes after initial acquisition by the sensors. At 5.5 minutes after epoch the two tracks begin to diverge because tracking in the 30°-90° scenario has stopped but tracking continues in the 30°-30° scenario. In general since tracking continues the estimated trajectory from the 30°-30° scenario will be more accurate.

Review of Figure 6 – Figure 11 indicate the range, azimuth and elevation cases are the most effective and could lead to a solution for an interceptor. Of the remaining cases, azimuth and elevation are the next best, but lack precision for an interceptor firing solution unless something is added to increase the precision.

Noteworthy in Figure 12 – Figure 15 is the fact that all radial positions seem to stabilize (stop oscillating from high to low) when the missile is closest to directly overhead. This is typical behavior of a sequential estimator since the estimator is beginning to converge after a sufficient number of observations. Additionally, the range, azimuth and elevation solution has the highest accuracy for determining position. The angles-only solution (azimuth and elevation) is next closest in merit to the range, azimuth, and elevation but still remains ~50 times larger at the worst point and in general is two orders of magnitude worse than the error of the range, azimuth and elevation solution.

Scrutiny of Figure 6 – Figure 11 shows that the range and range rate solution is only slightly better than the range only solution. This means that the range rate measurement is only slightly aiding the trajectory estimation. Note that the initial covariance of the range and range rate solution is smaller than that for the range only solution. This further indicates the range rate measurement yields

little efficacy in the estimation. This raises the question of what range rate accuracy is needed to significantly improve the trajectory estimation accuracy.

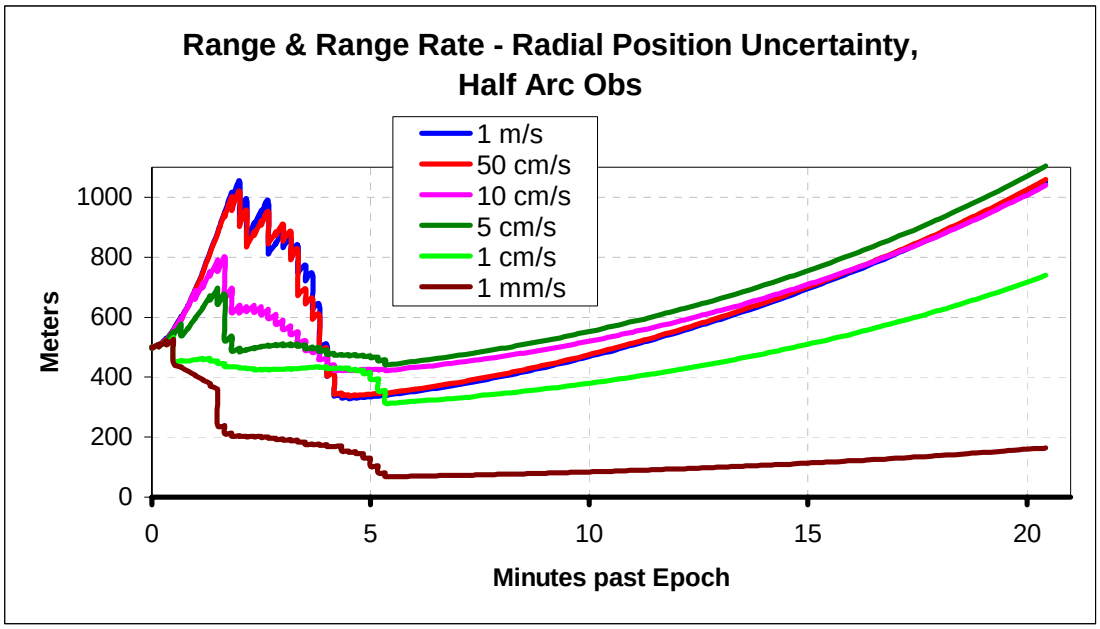

Figure 16: Radial Position Uncertainty with Range Rate Reduction

Figure 16 is a radial position uncertainty chart for range and range rate that shows a reduction of range rate sensor accuracy while range sensor accuracy remained at two meters/second. It can be seen from Figure 16 that in order for the range rate measurements to provide substantive help in estimating the missile trajectory, range rate error needed to be less than 0.005 % (times a constant) of the range error. Since this is not possible given the available range rate sensors, range rate comparisons were dropped from the dual site comparison.

Close examination of Figure 13 indicates the accuracy of position differenced range-only comparison half arc observation is better than the accuracy of the full arc solution. . This seems to be a statistical anomaly and will not be the norm. Comparison of the uncertainty plots, Figure 6 & Figure 7, show that, as expected, the full arc solution is better than the half arc solution.

Also tracked were the RIC differences and the 0.95p error bounds were plotted along the boundary. As seen in Figure 17 – Figure 19 below, positions remain within the 0.95p error bounds during all times. Assuming the data are from an approximately normally distributed population, the two sigma (2σ) confidence interval indicates 95.45% of the trajectories will pass within these bounds. The results of the range, azimuth and elevation solution are the only ones displayed for brevity, while other results were gathered and are similar; the other results are not displayed in this thesis. Figure 17 – Figure 19 reference the "missle" (not a misspelling, but a file name for the scenario) and reference 0.95 P positive and negative error bounds with a solid black line. Because the simulator was differenced with the filter, the reference position will always be zero and these solid black lines will be non-distinguishable with respect to the x axis.

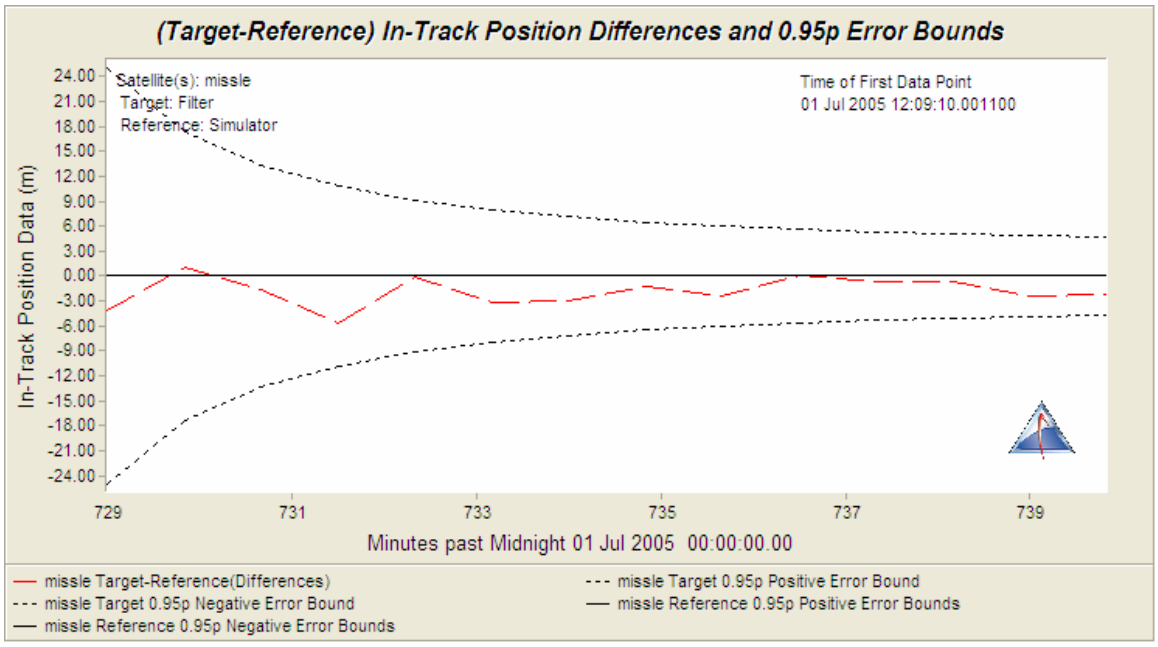

Figure 17: In Track Position Differences and 0.95p Error Bounds - Range Azimuth & Elevation

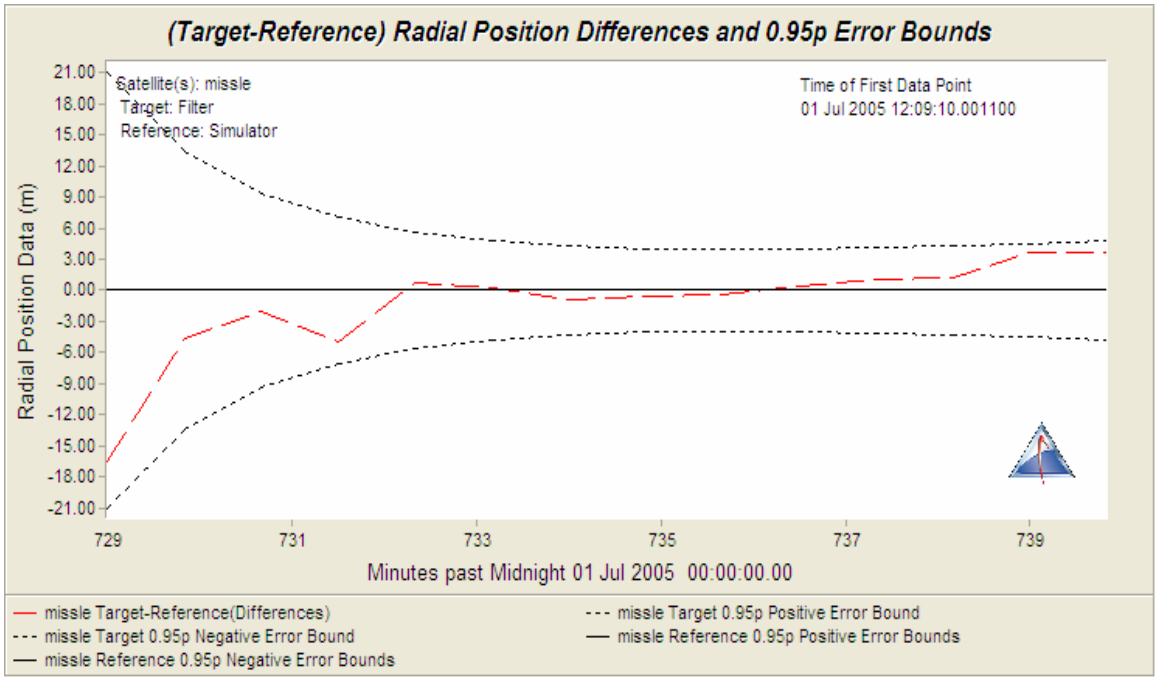

Figure 18: Radial Position Differences and 0.95p Error Bounds - Range Azimuth & Elevation

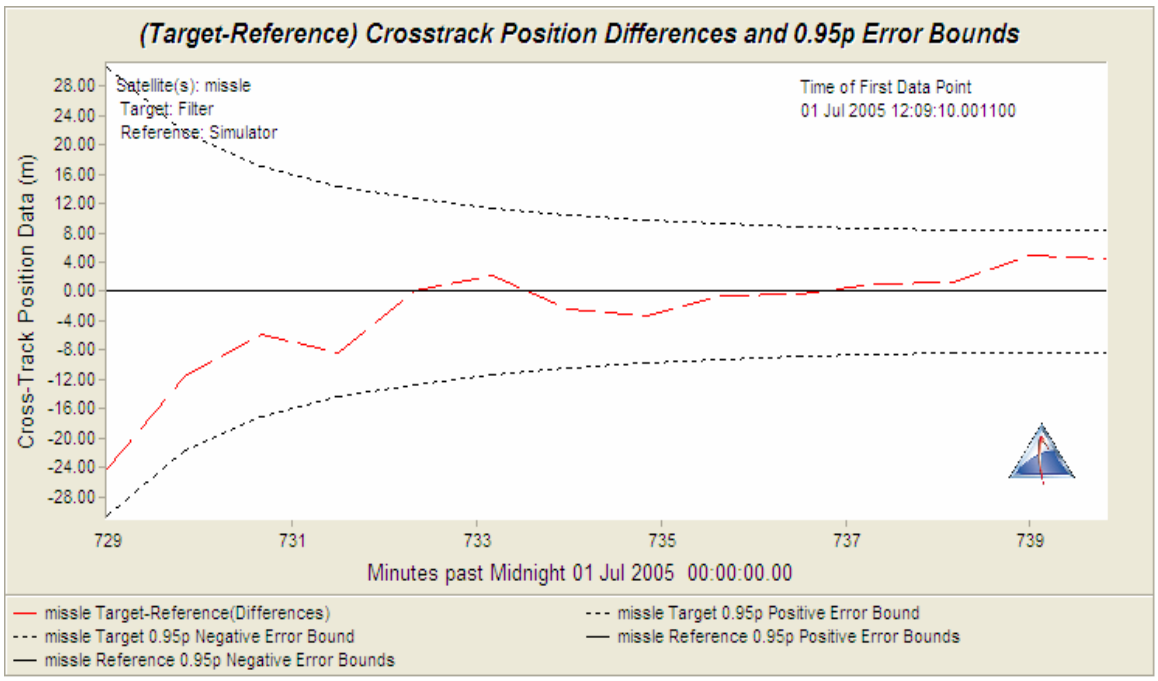

Figure 19: Cross Track Position Differences and 0.95p Error Bounds – Range, Azimuth & Elevation

The residuals are the difference between the measurement and the calculated measurement based on the estimated trajectory. Both methods of orbit determination, batch least squares and the Kalman filter, are designed to minimize the sum of the normalized residuals (or residual ratios), where the normalized residual is the residual divided by the measurement standard deviation. If the orbit determination was perfect and the sensor measurement statistics correctly modeled then the normalized residuals should have a mean of zero and a standard deviation of one. Thus, analysis of the normalized residuals is an indication of the quality of the fit and the accuracy of the sensor modeling. For example, if the standard deviation of the normalized range measurement was two and the bias was zero this would indicate that the modeled, or input, elevation angle standard deviation was likely half the actual value. Additionally if its mean was not zero this would indicate there is a bias. Note that since the residuals are a finite sized sample the mean will likely never be zero or the standard deviation exactly one. ODTK provides numerical outputs and plots of the residual ratios. These are from the filrun files and are represented in Figure 20 – Figure 23.

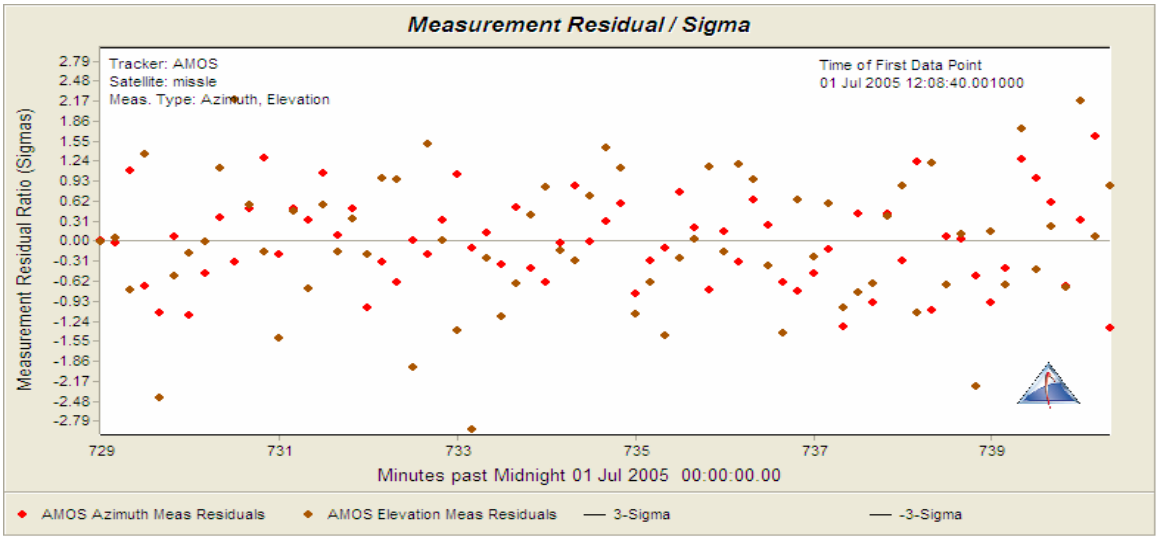

Figure 20: Residual ratios, Azimuth & Elevation Observations

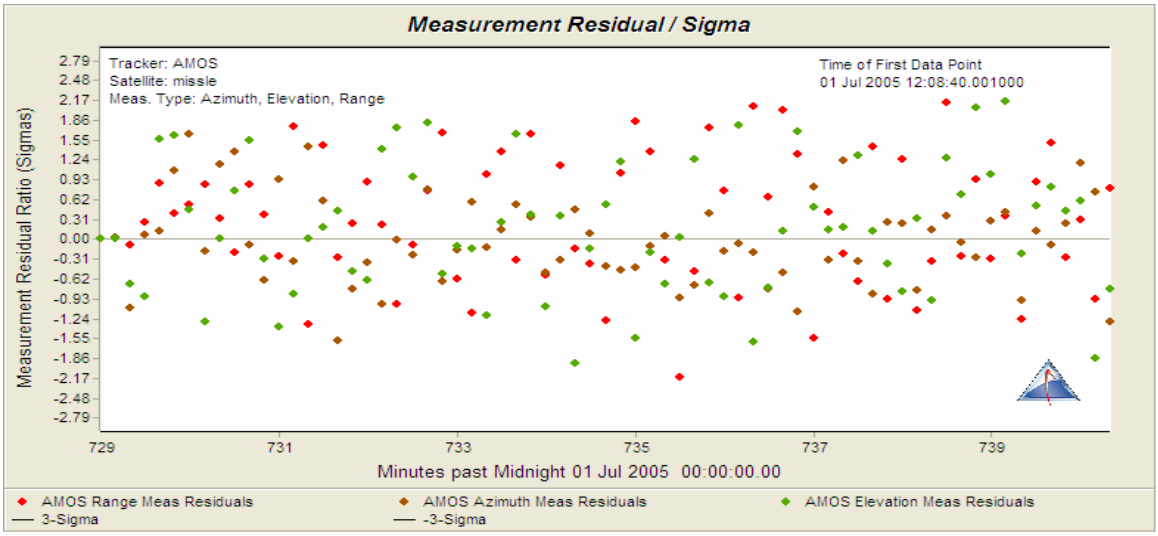

Figure 21: Residual Ratios, Range, Azimuth & Elevation Observations

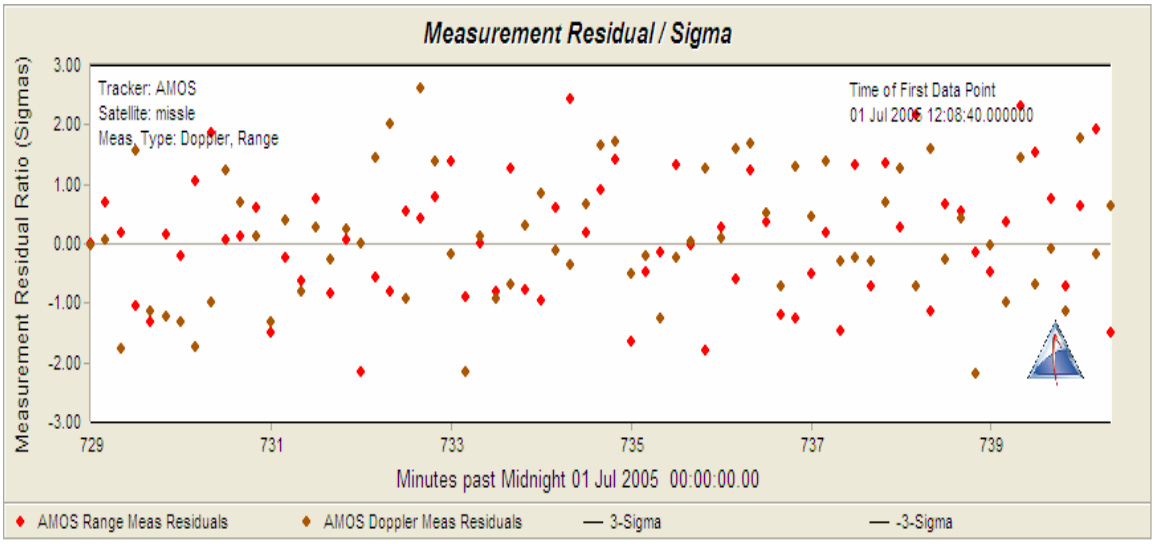

Figure 22: Residual Ratios, Range & Range Rate Observations

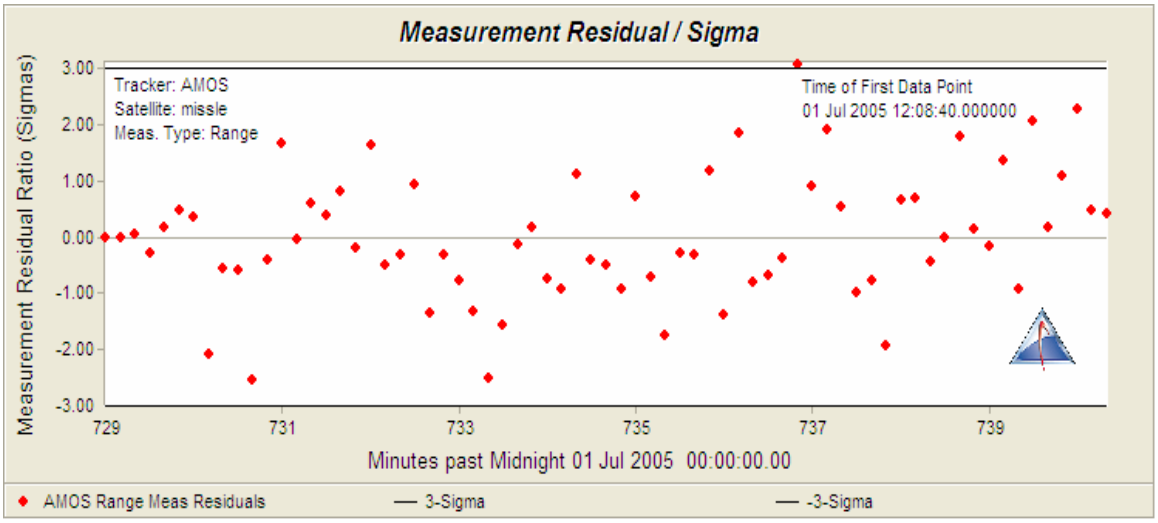

Figure 23: Residual Ratios, Range-Only Observations

Demonstrative of the uniformity of the data, the normalized mean and standard deviation for the range, azimuth elevation scenario are displayed in Table 5. Taking into account there were only 70 observations and the estimated trajectories are not exactly the truth trajectories, the values in Table 5 are indicative of correctly modeled sensor noise.

Table 5: Mean and Standard Deviation of Full Range Azimuth and Elevation Observations Scenario

	Normalized Mean	Standard Deviation
Range	.0305 meters	1.138478812
Azimuth	0.006 °	0.87713935
Elevation	0.169 °	1.188861353

In Figure 23, one residual slightly exceeds the 3σ boundaries (99.73% probability assuming the data are from an approximately normally distributed population) while all the other residuals are well behaved and remain with in the 3σ boundaries. This is a minimal and singular occurrence that strays outside the 3-sigma line showing the statistical probability of being in the 0.27 percentile.

B. MULTIPLE SITES

To achieve a better known initial position, a second site could be used to acquire the missile earlier in the trajectory. For instance, a SPY-1 capable ship can be assigned off the coast to observe and record the launch of a missile as shown in Figure 24. This sensor could track sooner because of geographic position and hand-off a more exact position of the missile. With a superb initial orbit, this section intends to prove the angles-only and range-only estimate could be as useful as the range and angles estimates for determining the orbit.

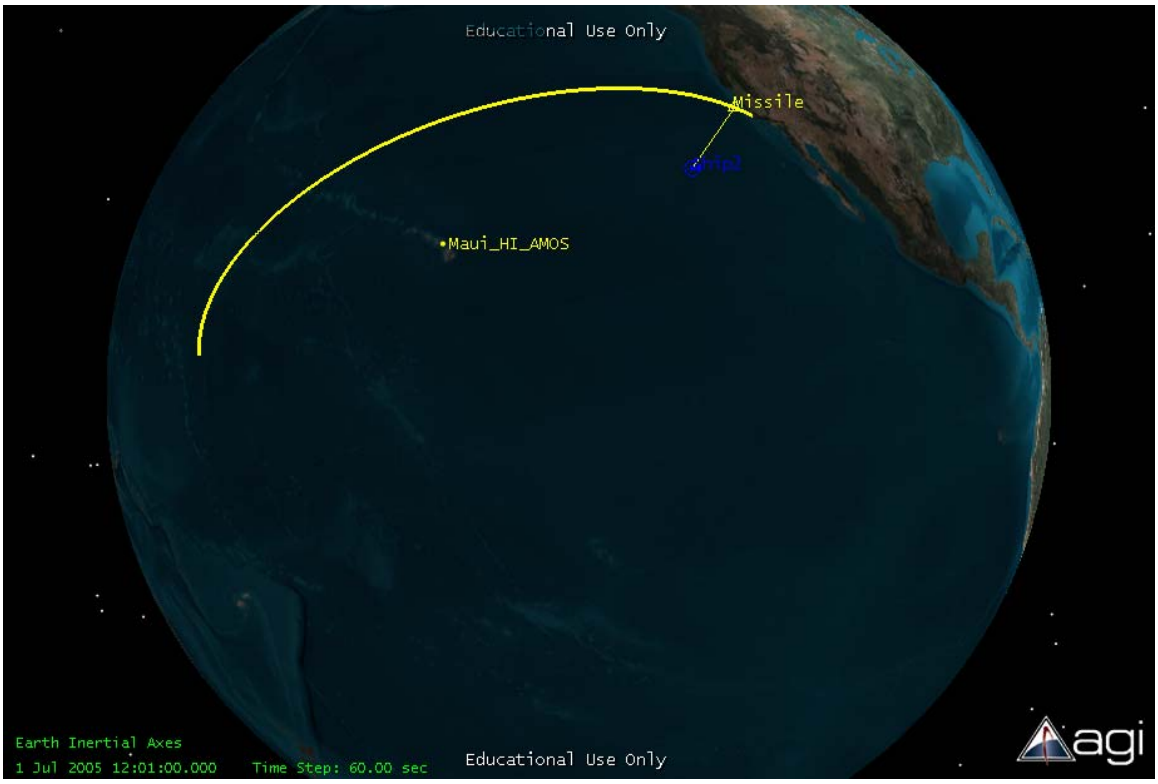

Figure 24: STK Visual of Ballistic Trajectory with a Ship Sensor

The same types of simulations were generated as were run for the single sensor case save the range and range rate case. The range and range rate case was not run in the dual site case because the range and range rate showed little efficacy unless the range rate accuracy was reduced to numbers smaller than possible given the available range rate sensor, and the efficacy was not demonstrated in the single site run.

The stated sensor errors for the ship site are; range resolution of five meters and an angular resolution of 540 microradians. These values are representative of space track radars, e.g., Eglin, not necessarily the Aegis. The Aegis frequency is much higher than the space track radar frequencies and consequently Aegis should be more accurate. As a result performance with the Aegis should be better than the results presented here. The actual values are classified and not available. The assumed measurement statistics are detailed in Table 6. Further assumed was the fact that the Aegis sensors cannot "see" the object until it is 30° above the observation point's horizon. The scenario was established such that Aegis stops tracking when the missile goes below 30° or when AMOS starts to see the missile, whichever comes first. While the second site was varied with respect to which sensors were used to track, the first site always used range, azimuth and elevation tracking sensors. Figure 28 – Figure 30 are identical in the first seven minutes of missile flight (approximately) because the same sensors are used in each scenario initially

Table 6: Measurement Statistics

	White noise sigma	Estimate Bias	Tropo Sigma	Light time delay
Range	5 m	False	0	True
Azimuth	.015 °	False	----	----
Elevation	.015°	False	.05	----

The position uncertainty for RIC given each scenario are displayed in Figure 25 – Figure 27. The radial, in-track and cross-track standard deviations of the four measurement scenarios allow us to draw conclusions from a statistically significant number of runs instead of just from one simulation. Details reports for the differenced radial position for each run are graphed in Figure 28 – Figure 30. These graphs show the single case results in the affirmative and these results coupled with the uncertainty data identify a strong case for all times and scenarios.

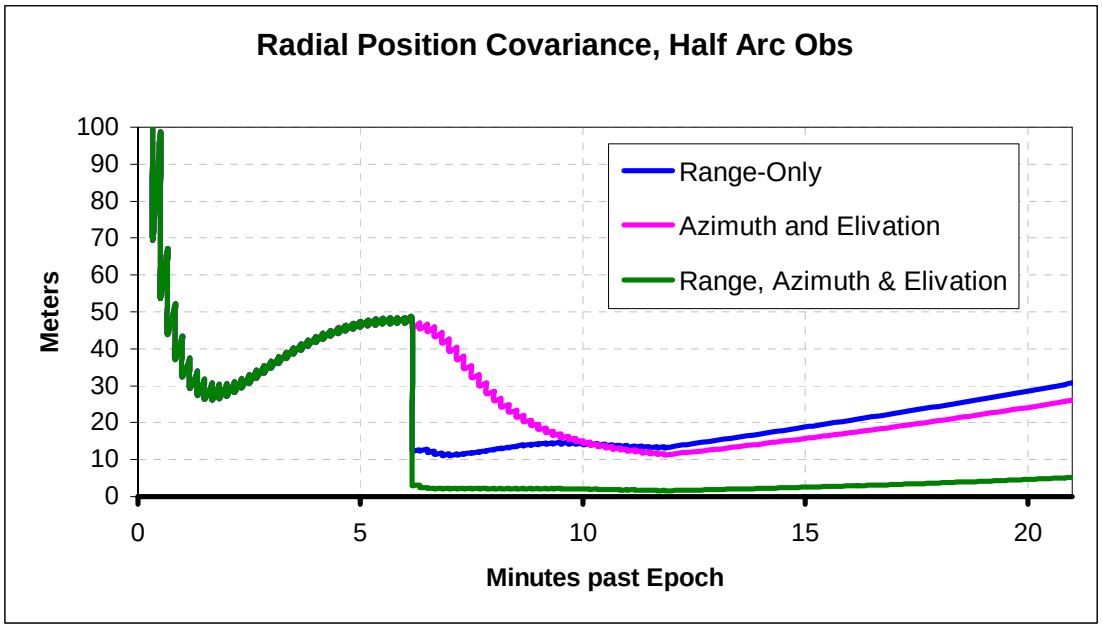

Figure 25: Dual Site, Radial Position Covariance, Half Arc Observations

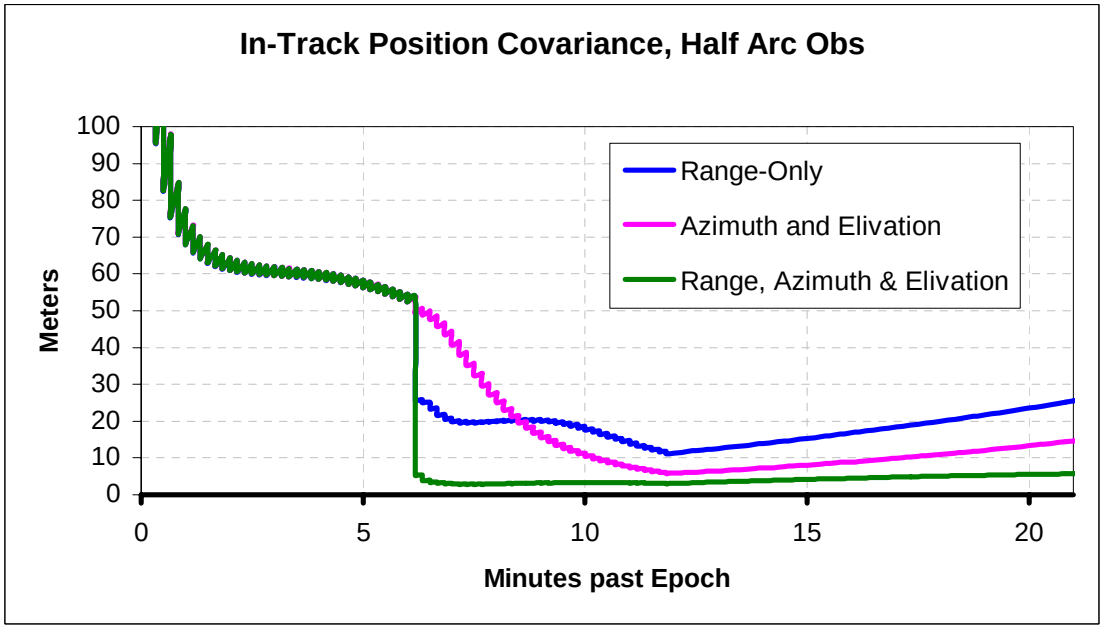

Figure 26: Dual Site, In-Track Position Covariance, Half Arc Observations

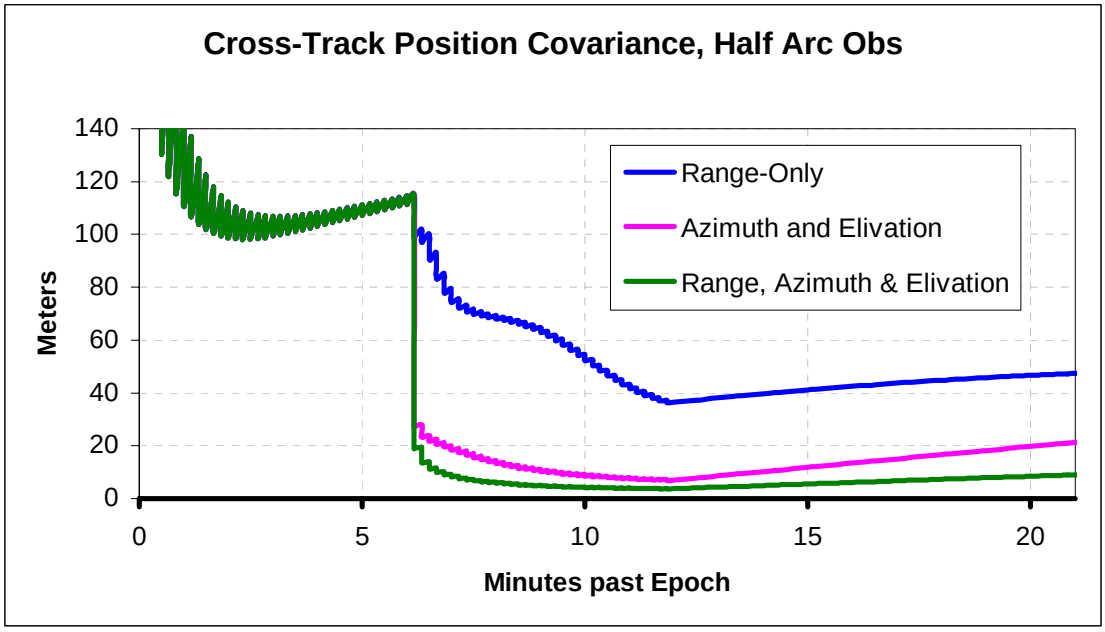

Figure 27: Dual Site, Cross-Track Position Covariance, Half Arc Observations

The first six minutes of the position covariance data in Figure 25 – Figure 27 indicate a single line for range, azimuth and elevation without the appearance of the other sensor combinations. While this line appears single, the data in range-only, azimuth and elevation as well as range, azimuth and elevation are identical during the time that the Aegis ship is tracking the missile.

As can be seen in Figure 28 – Figure 30, the same radial difference positions were graphically compared. As seems evident, the second site allowed for longer tracking of the object. The additional tracking time facilitated a better known initial position and when the ship's sensor handed off to the AMOS sight, the position was pin-pointed immediately. The difference in these graphs from those presented before in a similar fashion is these graphs contain both the differenced radial position from the single sensor and the dual sites. The single site does not begin to detect until approximately seven minutes after the ship detects the missile because of geographic position and is pictured in the same color as was done previously.

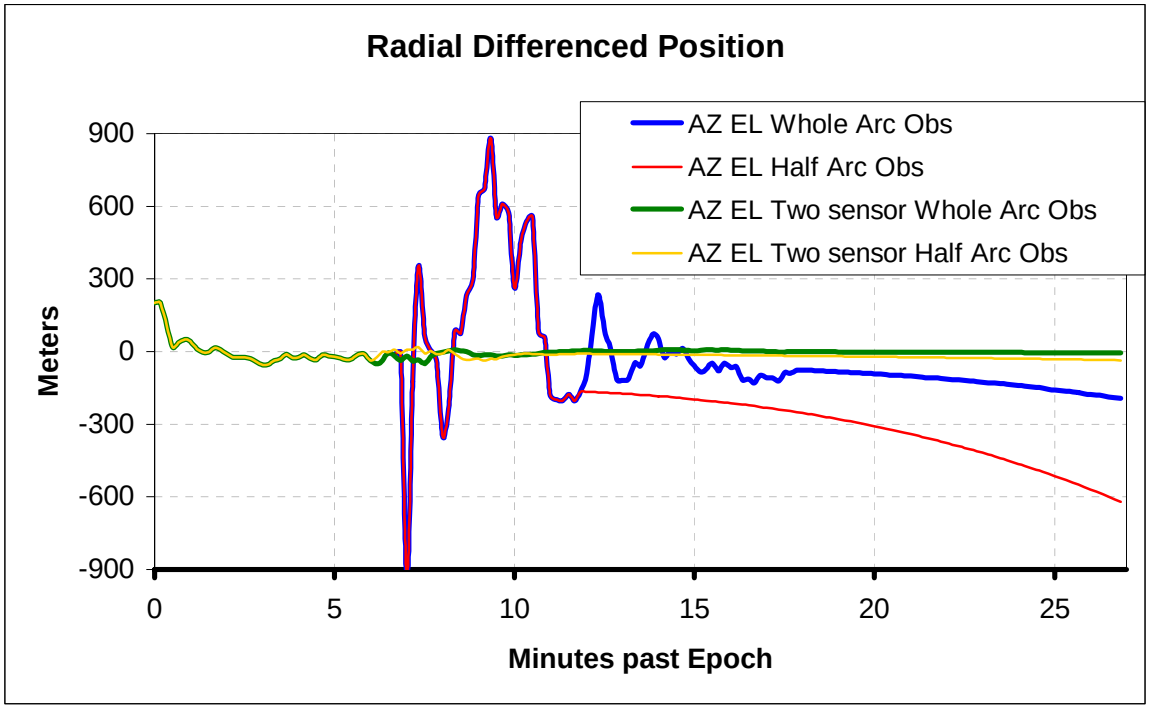

Figure 28: Differenced Radial Position for Azimuth & Elevation Observations at Maui

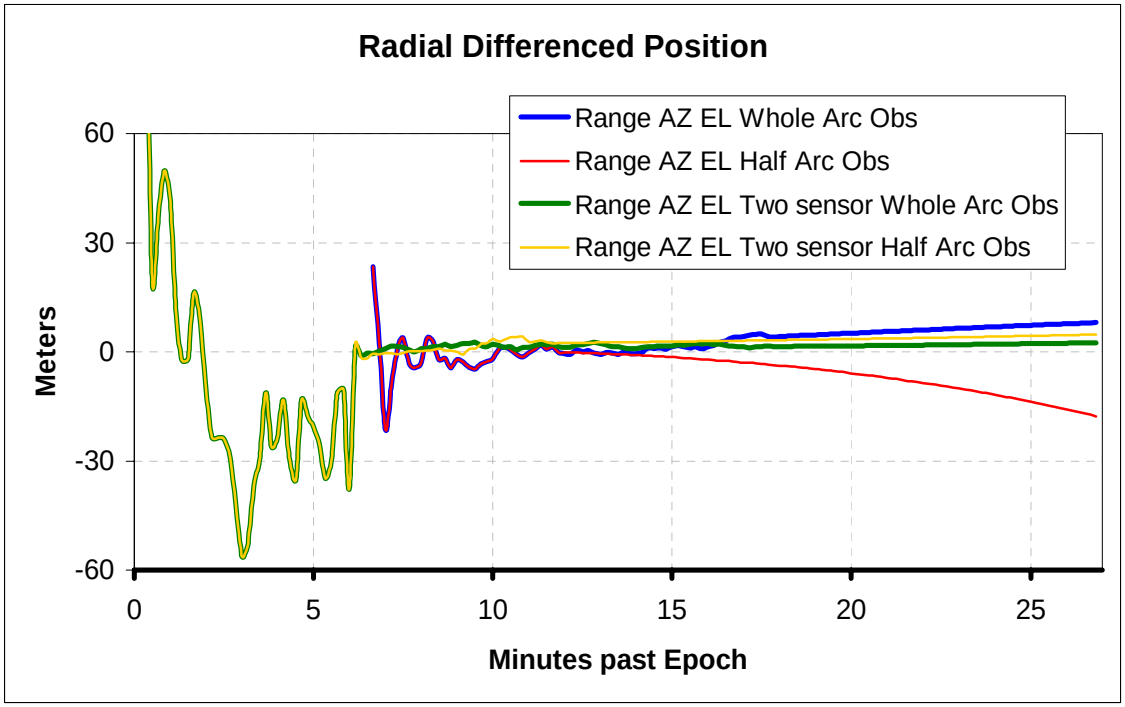

Figure 29: Differenced Radial Position for Range, Azimuth & Elevation Observations at Maui

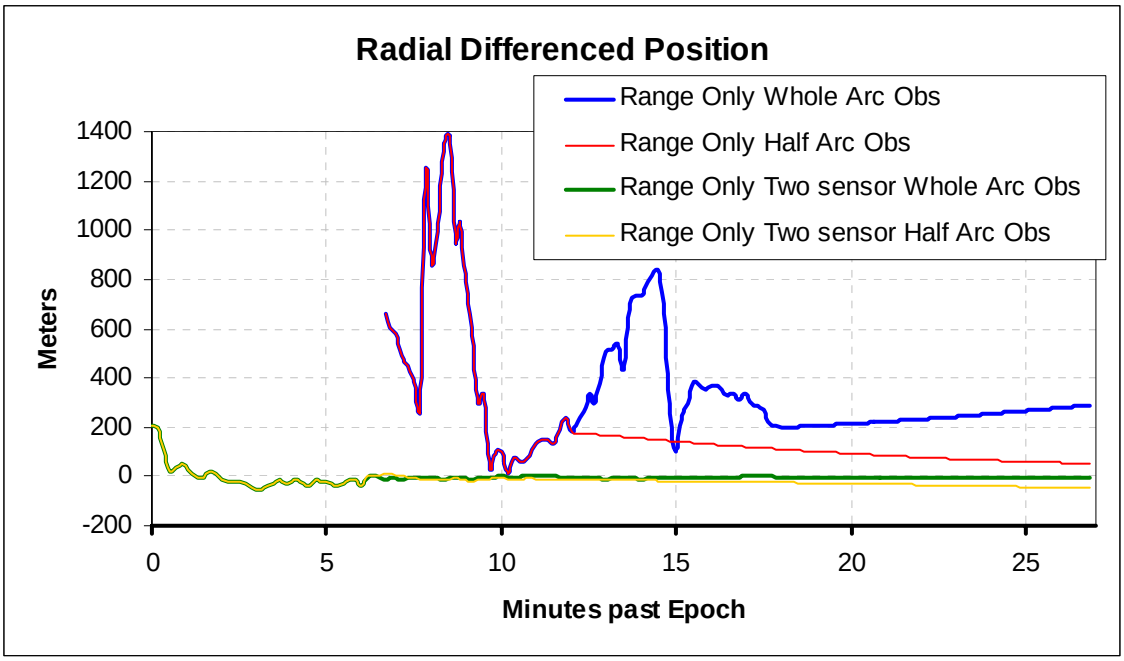

Figure 30: Differenced Radial Position for Range-Only Observations at Maui

Figure 28 shows the observations with the two sites yielded better performance, which was at times a full order of magnitude better than the performance with a single site when using angles-only at the second site. The addition of a geographically earlier second site allows the primary site to use azimuth and elevation, which was previously not considered a viable method for tracking an in bound missile.

Figure 29 represents the range, azimuth and elevation observations. As seen previously, the single site results were very good and it was considered a viable method for tracking an in bound missile. The addition of the second site improved the fidelity of the observations by between two and up to five times over the single site observations.

Figure 30, which represents the range-only observations with the two sites yielded better performance which was at times three orders of magnitude better than those observations with a single site. The second site allows range-only observations to be considered a viable method for tracking an in bound missile.

It is also noteworthy that the difference between the full arc observations and half arc observations is considerably less on the scenario with a single site. The dual site has differences that are between four and six times more between half arc and full arc coverage as opposed to between two and four times more (or less in the case of range) for the single site. The tracking accuracy achieved with two sites in all three measurement scenarios with tracking ending at maximum elevation should be sufficient for handoff for an interceptor.

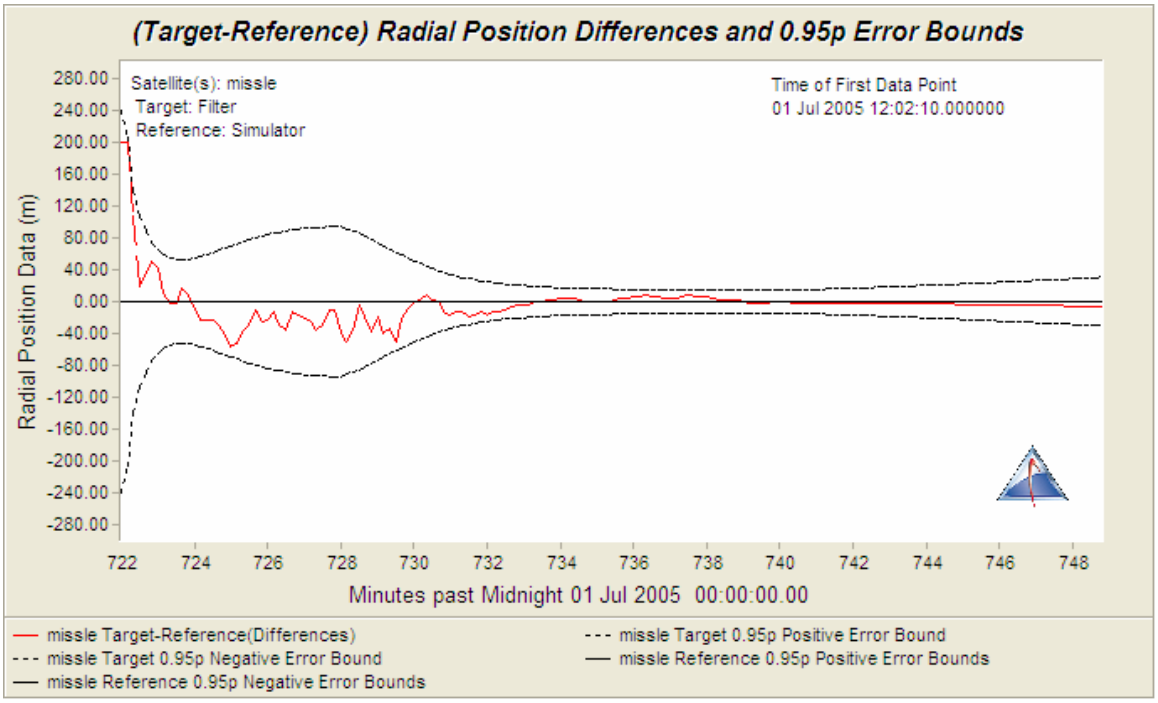

Figure 31: Radial Position Differences and 0.95p Error Bounds – Azimuth & Elevation

Noteworthy in Figure 32 and Figure 33 is the immediate decrease in the 0.95 P error bounds with the occurrence of the second site acquiring the target. This indicates the position is very well known after acquisition. In these two figures, it is easy to see that the trajectory does not exceed the o.95P bound. Figure 31 and Figure 33 show a similar decrease in the 0.95 P boundaries at acquisition of the second site, but the boundaries do not decrease to near zero, as is the case on Figure 32. Additionally, Figure 31 and Figure 33 show a similar final performance, which indicates the azimuth and elevation performance is

similar to the range-only in the radial direction. This is probably because the range, azimuth and elevation observations pin point the position so well.

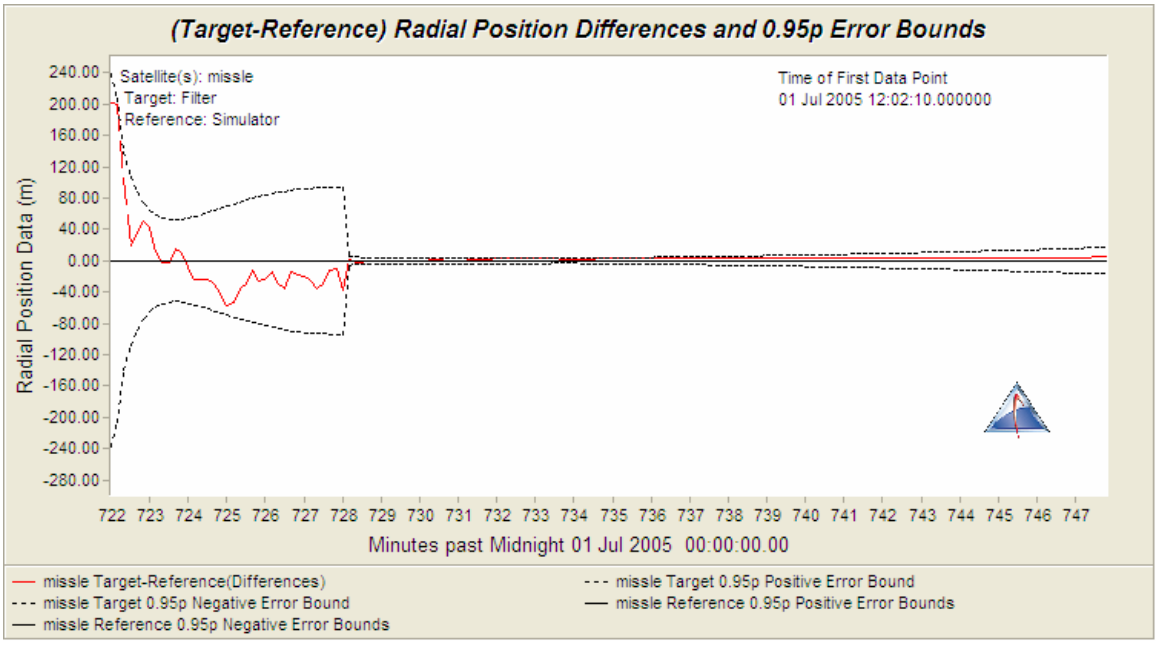

Figure 32: Radial Position Differences and 0.95p Error Bounds – Range, Azimuth & Elevation

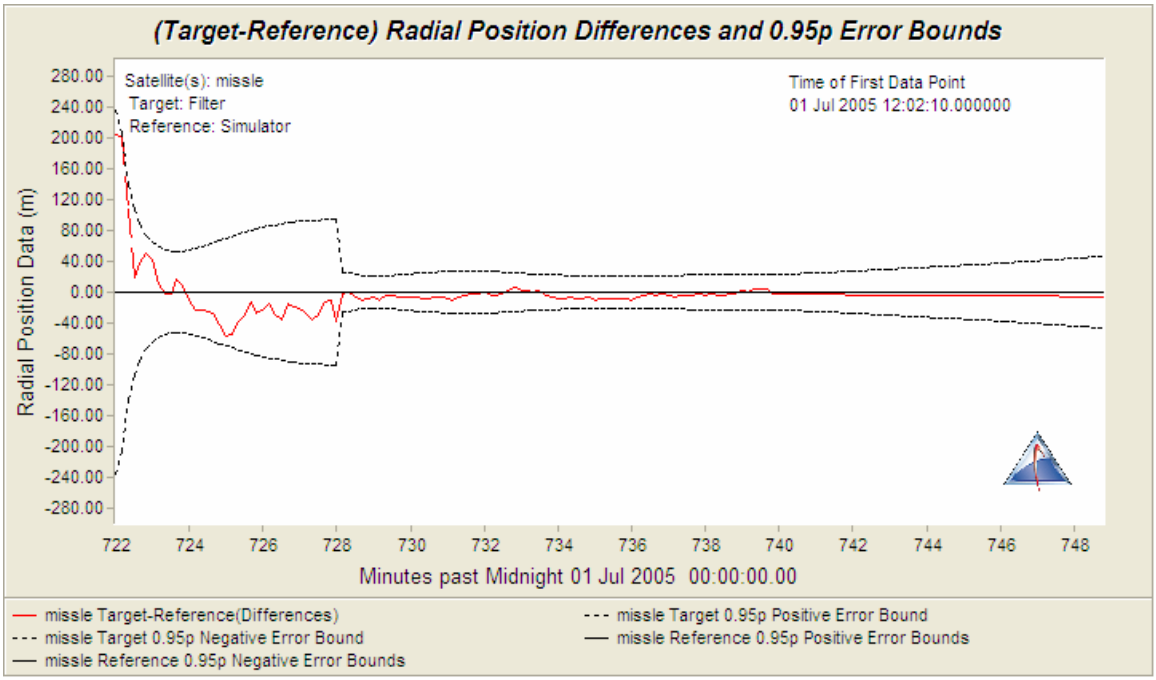

Figure 33: Radial Position Differences and 0.95p Error Bounds – Range-Only

As stated previously, the residuals are the difference between the measurement and the calculated measurement based on the estimated trajectory. The results of the residual ratios are pictured in Figure 34 – Figure 36. A clear line of demarcation can be seen upon site two acquisition with the color change of the residuals.

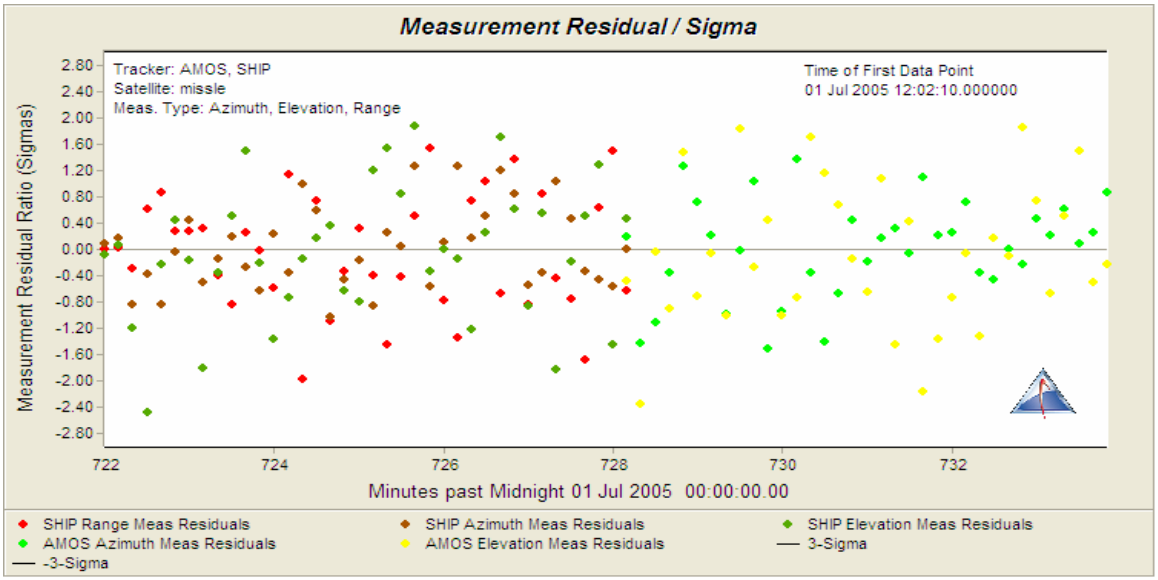

Figure 34: Residual Ratios Dual Sites, Azimuth & Elevation at Maui

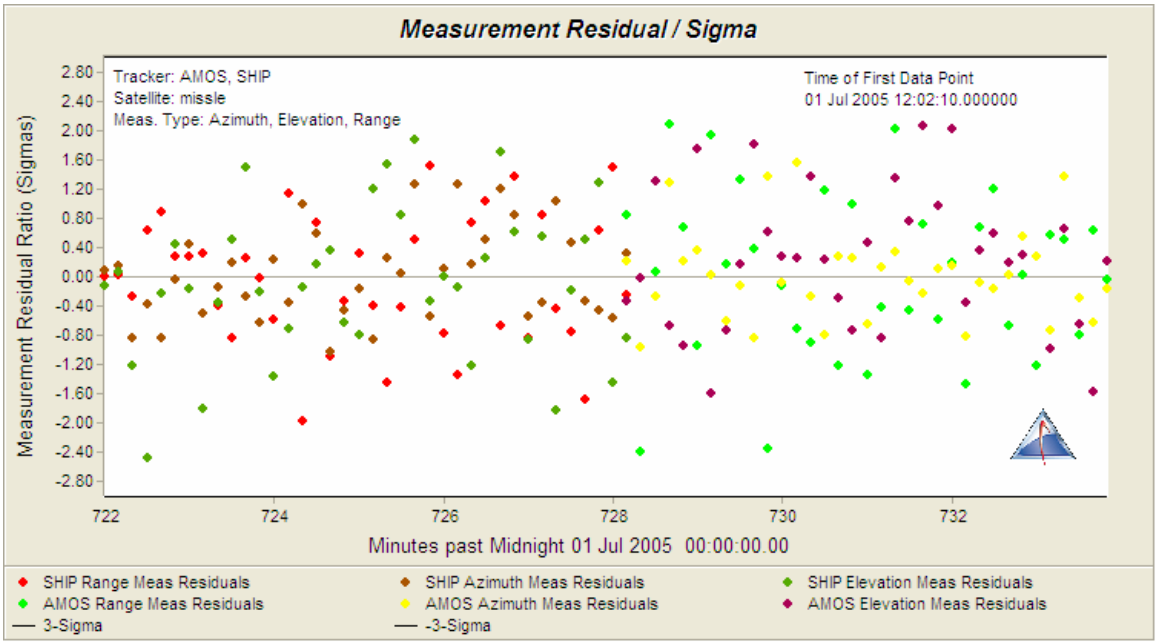

Figure 35: Residual Ratios Dual Sites, Range, Azimuth & Elevation at Maui

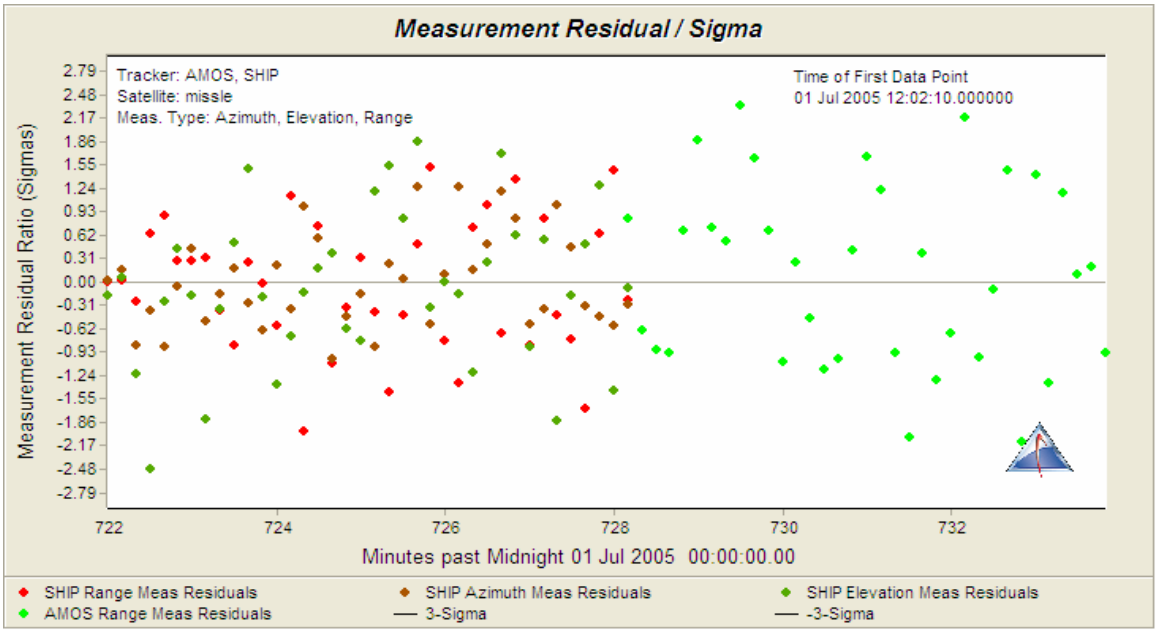

Figure 36: Residual Ratios Dual Sites Range-Only

Visually represented in Figure 37 – Figure 38 are the position uncertainties of the missile. The cases represented contain Radial, In-track and Cross-track position uncertainty and are both pictured for the angles-only case for like comparison. The uncertainty of the position decreases significantly with the introduction of the site. Note the time difference in the time for both scenarios. The dual site scenario generates a reasonably small position uncertainty with the initial site, but as soon as the second site acquires, the position uncertainty drops. Contrarily, the single site case has a saw tooth type of reduction of position uncertainty which takes a few minutes to reduce to usable levels. Other cases of angles-only and range-only have similar but exaggerated differences.

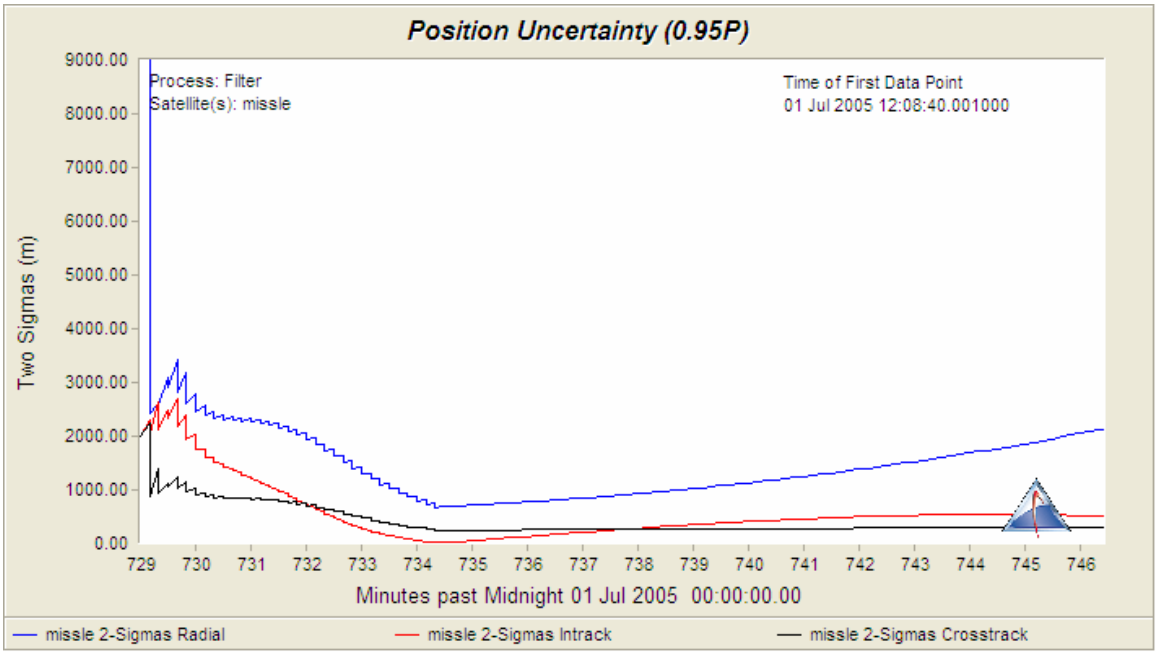

Figure 37: Position Uncertainty for Single Site

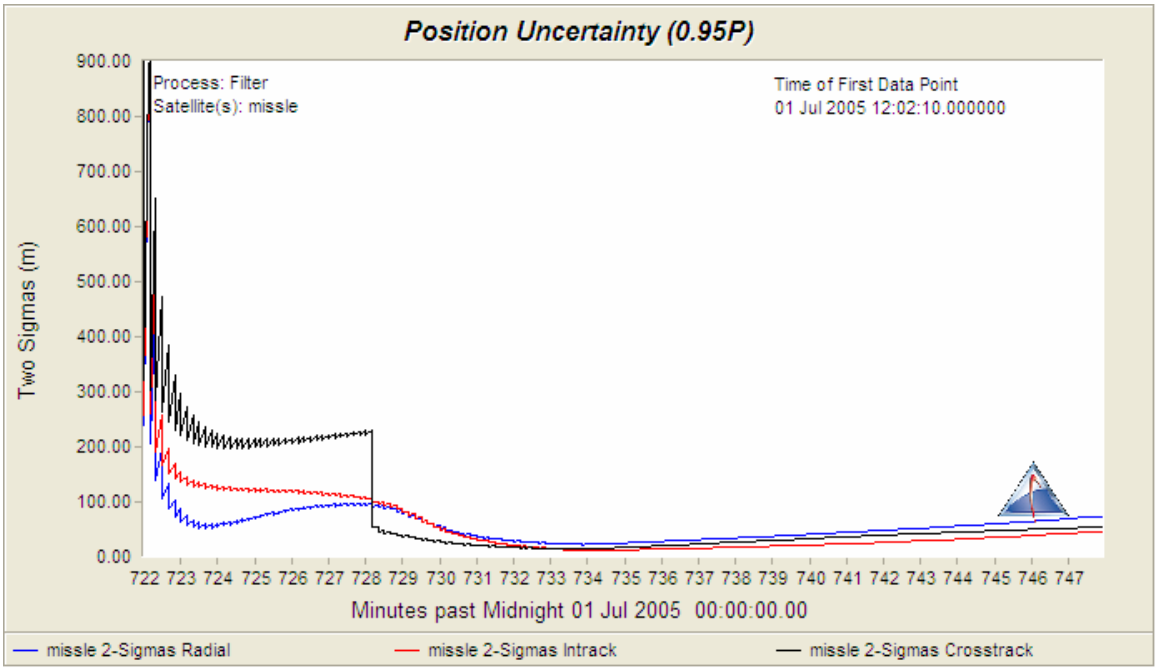

Figure 38: Position Uncertainty for Dual Site

V. CONCLUSIONS

This thesis investigated and compared the accuracy of a ballistic missile trajectory using four types of measurements: range-only; range, azimuth and elevation; azimuth and elevation; as well as range and range rate. Sensor measurements are commensurate with current values of telescopes and laser ranging systems. Further investigated was the use of two sites vs. a single site as well as the usefulness of 30°-30° observations as well as 30°-90° observations for both types of sites. Waiting to determine the orbit until the 30° downward trajectory is less than ideal because at the time of the last observation, the object has almost impacted its intended target.

As expected, the range, azimuth and elevation measurement system resulted in the best trajectory determination and prediction. Using angles-only, range-only as well as range / range rate measurements does not provide sufficient trajectory prediction accuracy for a single sensor. It has also been determined in order for the range rate measurements to provide substantive help in estimating the missile trajectory, range rate error needed to be less than 0.005 (times a constant) of range measurement error. This increase in sensor accuracy is not possible with present range rate sensors.

During the 30°-90° scenario for both the single site and the two site scenarios, the position error drift ranged from minimal to significant predicated on the accuracy of the state at the last observation. It was found that the combination of range, azimuth and elevation sensor data until the ~90° point yields an orbit determination that has enough merit to hand-off to an interceptor.

It was found that the dual sites increase the fidelity of the angles-only and range-only measurements such that the combination of azimuth and elevation or range only sensor data yields an orbit update that is sufficient to hand-off to an interceptor even if using the 30°-90° observations. The second sensor yielded 5.5 minutes more tracking time which refined the orbit enough to be consistent with the original range, azimuth and elevation measurement system.

THIS PAGE INTENTIONALLY LEFT BLANK

VI. FUTURE WORK

As described in the introduction, the re-entry vehicle may break into six or more separate warheads at some time after the projectile becomes ballistic. These warheads may be targeted at a single location or multiple locations. Using the concept herein, a potential future objective could be to focus on the use of differential angles data in determining the motion of multiple Reentry Vehicles (RVs) relative to a primary RV that is being accurately tracked. This could hasten the identification of dummy warheads.

Additional follow on work could include running the smoother on ODTK for all the orbit determinations to backward calculate the exact orbit without the presence of errors and with the knowledge of the complete trajectory. Since this sensor platform is fixed, the concept in this thesis could be applied to a moving sensor platform.

THIS PAGE INTENTIONALLY LEFT BLANK

APPENDIX: ODTK SCENARIO SETTINGS

1. FACILITY (AMOS)
- Position Geodetic
  - Lat — 20.7084 deg
  - Lon — -156.257 deg
  - Alt — 3059.5 m
- Tracking ID — 100
- Estimate — Nothing
- MinElevation — 30 deg
- MaxElevation — 90 deg
- RangingMethod — Transponder
- AntennaType — Mechanical
- Optical Properties
  - PolarExclusion — 1 deg
  - ReferenceFrame — MEME J2000
  - AberrationCorrections — None
- TroposphereModel
  - Enabled — Based on Tracking System
  - Model — SCF
- TroposphereData
  - SurfaceRefractivity — Constant
  - Value — 340
- IonosphereModel
  - Enabled — Based on Tracking System
  - Model — IRI2001
  - TransmitFreq — 2267.5MHz
  - ReceiveFreq — 1815.77MHz

2. FACILITY (SHIP)
- Position Geodetic
  - Lat — 34.6 deg
  - Lon — -133 deg
  - Alt — 0 m
- Tracking ID — 101
- Estimate — Nothing
- MinElevation — 30 deg
- MaxElevation — 90 deg
- RangingMethod — Transponder
- AntennaType — Mechanical
- Optical Properties
  - PolarExclusion — 1 deg
  - ReferenceFrame — MEME J2000
  - AberrationCorrections — None
- TroposphereModel
  - Enabled — Based on Trackin System
  - Model — SCF
- TroposphereData
  - SurfaceRefractivity — Constant
  - Value — 340
- IonosphereModel
  - Enabled — Based on Tracking System
  - Model — IRI2001

- TransmitFreq 2267.5MHz
- ReceiveFreq 1815.77MHz

3. INITIAL ORBIT DETERMINATION (IOD)
- Method Herick / Gibbs
  - Selected Facility SHIP
  - Measurement Pass 1
  - MeasurementSampleSize 300
  - MinimumElevation 30 deg
  - SelectedMeasurments Double click to edit
- Output
  - OrbitState Cartesian
  - CoordinateFrame J2000
  - EPOCH 1 Jul 2005 12:02:10.000 UTCG
  - XPosition 5009.51 km
  - YPosition -2660.92 km
  - ZPosition 3772.53 km
  - XVelocity 0.400538 km^sec^-1
  - YVelocity -5.92701 km^sec^-1
  - ZVelocity 0.840157 km^sec^-1

4. FILTER
- ProcessControl
  - StartMode Initial
  - StartTime 1 Jul 2005 12:02:10.000 UTCG
  - StopMode StopTime
  - StopTime 1 Jul 2005 12:29:06.480 UTCG
  - ProcessNoiseUpdateInterval 10 sec
- OptionalSolveForParms
  - MeasBiases false
- Output
  - DataArchive
    - OutputStateHistory AllTimes
    - EveryNSteps 1
    - SaveOnlyLastMeasPerStep false
    - OutputMeasHistory true
    - OutputManeuvers true
    - OutputSummary true
    - OutputHistograms true
    - HistogramSize 3
    - NumberHistorgramBins 22
  - Display
    - EveryNMeasUpdates 1
    - EveryNTimeUpdates 1
    - ShowPassTimes true
  - SmootherData
    - Generate false
  - STKEphemeris
    - DuringProcess
      - Generate true
      - Time Grid Filter
    - Predict
      - Generate false
    - Generate false
    - Covariance true

        - Covariance type — Position 3x3 Covariance
        - EVENTS — Output all

5. SIM
    - Meas Types — Double click to edit
    - Start time — 1 Jul 2005 12:00:00.000 UTCG
    - Stop time — 1 Jul 2005 12:29:06.480 UTCG
    - Time step — 10.000000000000000 Sec
    - Custom tracking intervals
        - Enabled — True
            - Schedule
                - Specific tracker — AMOS
                    - 12:08.20.000 – 12:14.01.000 (Half)
                    - 12.08.20.000 – 12:29:06.480 (Full)
                - Specific tracker — SHIP
                    - 12:00:00.000 – 12:08.20.000
    - Error Modeling
        - No Deviations — false
        - Deviate Orbits — false
        - Deviate density — false
        - Deviate B COeff — false
        - Deviate SolarP — false
        - Deviate measurmentbias — false
        - Deviate Manuouvers — false
        - AddProcess Noise — false
        - AddManouverProcess Noise — false
        - AddGPSReceiver ClockPrcessNoise — false
        - AddMeasWhiteNoise — true
        - DevaiateStationLocations — false
        - Random Seed — 1
        - Error Scaling
            - Orbits — 1
            - Density — 1
            - BCoeff — 1
            - SolarP — 1
            - TranspDelay — 1
            - MeasurBias — 1
            - Manouvers — 1
            - StationLocations — 1
        - Update Filter times — true
        - Output
            - DataArchieve
                - Every N Step — 1
                - Histogram size — 3
                - NumberHistgramBins — 22
                - Outputperterbations — true
            - STK Ephemeris
                - Generate — true
                - Acceleration — false

6. SATELLITE (MISSLE)
    - Description
    - OrbitState — Cartesian
    - EPOCH — 1 Jul 2005 12:02:10.000 UTCG
    - XPosition — 4900.49 km

- YPosition -1863.06 km
- ZPosition 3620.28 km
- XVelocity 1.29992 km^sec^-1
- YVelocity -6.33318 km^sec^-1
- ZVelocity 1.51314 km^sec^-1
- EstimateOrbit true
- OrbitClass UNDEFINED
- PhysicalProperties
  - Mass 1000 kg
- MeasurementProcessing
  - TrackingID 1001
  - MeasurementTypes Range, Range Rate, Azimuth Elevation
  - ResidualEditing
    - NominalSigma 3
    - Dynamic
      - Enabled false
      - HighSigma 100
      - NumRejectToStart 10
      - NumAcceptToStop 3
      - InitialHighSigmaDuration 0 min
  - ThinningTime 0 sec
  - MinPassDelta 20 min
- MeasurementStatistics None
- MinGrazingAlt 100 Km
- OpticalProperties
  - PolarExclusion 1 deg
  - ReferenceFrame MEME J2000
  - AberrationCorrections None
- RangingMethod Transponder
- IonosphereModel
  - Enabled false
- ForceModel
  - Gravity
    - DegreeandOrder 21
    - Tides
      - SolidTides false
      - OceanTides false
    - GeneralRelativityCorrection false
    - VariationalEquations
      - Degree 2
    - ProcessNoise
      - Use BasedOnOrbitClass
      - WillUseProcessNoise false
      - OmissionErrorModeling
        - Enabled true
        - Scale 1
      - CommissionErrorModeling
        - Enabled true
        - Scale 1
      - ThirdBodies
        - Sun true
        - Moon true
        - Planets false
        - UseinVariationaEquations false

- Drag
  - Use: No
  - WillUseAirDrag: false
- SolarPressure
  - Use: BasedOnOrbit
  - WillUseSolarPressure: true
  - EstimateSRP: true
  - CPNominal: .075
  - Area: 20 m^2
  - CPInitialEstimate: -3.79122e-007
  - CPSigma: 0.2
  - CPHalfLife: 2880 min
  - ReflectionModel: Sphere with perfect
  - SunPosMethod: ApparentToTrueCB
  - UseInVariationalEquations: false
  - AddProcessNoise: false
- Plugin
  - Use: false
- UnmodeledAccelerations
  - ProcessNoise
    - RadialVelocitySigma: 0 cm*sec^-1
    - IntrackVelocitySigma: 0 cm*sec^-1
    - CrosstrackVelocitySigma: 0 cm*sec^-1
    - TimeInterval: 2 min
  - InstantManeuvers: InstantManeuvers
  - FiniteManeuvers: FiniteManeuvers
  - OrbitErrorTransitionMethod: VariationalEquations

- PropagatorControls
  - IntegrationMethod: RK 4
  - StepSize
    - Time . : 10.0000000000000 sec
    - TrueAnomaly: 2 deg
    - EccentricityThreshold: 0.04
- EphemerisGeneration
  - CreateSTKFile: true
    - Span: 1440 min
    - Time Step: 10.0000000000000 sec
- OrbitUncertainty
  - R_Sigma: See Table 3
  - I_Sigma: See Table 3
  - C_Sigma: See Table 3
  - Rdot_Sigma: See Table 3
  - Idot_Sigma: See Table 3
  - Cdot_Sigma: See Table 3
  - AllCorrelations: 0
- FilterEvents
  - MeasurementRejectThreshold
    - NumForWarning: 0
    - NumForAlert: 0
  - MeasurementAcceptTimer
    - TimeGapForWarning: 0 min

TimeGapForAlert: 0

THIS PAGE INTENTIONALLY LEFT BLANK

LIST OF REFERENCES

1. Vallado, David A., *Fundamentals of Astrodynamics and Applications*, 2nd Edition, Microcosm Press, 2004
2. OD Tool Kit: A Technical Summary, 4th edition, v.3, 2004
3. Choset, Lynch, Hutchinson, Kantor, Brugrard Kavraki and Thrun, P*rinciples of Robot Motion,* MIT Press 2005
4. STK/ODTK manual, Analytical Graphics Inc., February 2006
5. Hill, K.C., Sabol, C., McLaughlin, C, Luu, K.K. and Murai, M., "Relative Orbit Determination of Geosynchronous Satellites Using the COWPOKE Equations," Paper No. AAS 04-195, AAS/AIAA Space Flight Mechanics Conference, Maui, HI, February 2004.

THIS PAGE INTENTIONALLY LEFT BLANK

INITIAL DISTRIBUTION LIST

1. Defense Technical Information Center
   Ft. Belvoir, Virginia

2. Dudley Knox Library
   Naval Postgraduate School
   Monterey, California

3. Dr. Chris Sabol
   Air Force Research Laboratory
   Kihei, Hawaii

4. Analytical Graphics, Incorporated
   Valley Creek Corporate Center
   Exton, Pennsylvania